



Review Article

Correlation between corrosion inhibitive effect and quantum molecular structure of Schiff bases for iron in acidic and alkaline media

*¹Loutfy H. Madkour and ²EiroybySK

¹Department of Chemistry, Faculty of Science and Arts, Baljarashi, Al-Baha University, P.O. Box1988 Al-Baha, Saudi Arabia

²Department of Chemistry, Faculty of Science, King Abdul-Aziz University, P.O. Box 80203 Jeddah 21589 Saudi Arabia

*Corresponding E-mail address: loutfy_madkour@yahoo.com, Tel. +966 541945518; Fax: +966 77247272

Accepted 14 December 2014

Abstract

Quantum chemical calculations using the density functional theory (DFT) have been applied to the five kinds of polydentate Schiff base compounds (PSCs), act as inhibitors for iron in aerated 2.0 M HNO₃ and 2.0 M NaOH media. The structural parameters, such as the frontier molecular orbital energy HOMO (highest occupied molecular orbital), LUMO (lowest unoccupied molecular orbital), energy gap ΔE ($E_{LUMO} - E_{HOMO}$), the charge distribution, the absolute electronegativity (χ), the fraction of electrons transfer (ΔN) from inhibitors to iron, the dipole moment (μ), the global hardness (η) and the total energy (E_{total}) were also calculated and correlated with their inhibition efficiencies (%IE). The inhibition effects of (PSCs) may be explained in terms of electronic properties. The results showed that the (%IE) of PSCs increased with the increase in E_{HOMO} and decrease in $E_{LUMO} - E_{HOMO}$. The inhibitor molecules were first adsorbed on the iron surface and blocking the reaction sites available for corrosive attack; and the areas containing N and O atoms are most possible sites for bonding by donating electrons to the iron surface through interaction with π -electrons of the aromatic rings, and the azo methine group. Also, the adsorbed Schiff base molecules interact with iron ions in the corrosive media leading to neutral and cationic iron-Schiff base complexes. Adsorption process is spontaneous, exothermic and obeyed Temkin isotherm and regarded as physical as chemical mechanism. The polarization studied indicated that the inhibitors act as a mixed type inhibitor in HNO₃; cause only inhibition of the cathode process in NaOH, and the magnitude of the displacement of the Tafel plot is proportional to its concentration. Models for the inhibition corrosion behaviour were developed based upon statistical analyses of the experimental data. Some thermodynamic and kinetic parameters (K_{ads} , ΔG_{ads}) were estimated. Both experimental and quantum theoretical calculations are in excellent agreement. The inhibition efficiency increase in the order of: PSC₁ > PSC₂ > PSC₃ > PSC₄ > PSC₅. Thus, DFT study gave further insight into the mechanism of inhibition action of PSCs. This research might provide a theoretical inhibition performance evaluation approach for homologous inhibitors.

Keywords: Corrosion inhibitor, Quantum chemical, DFT method, Schiff bases adsorption, Molecular orbital, Iron electrode, Temkin isotherm

INTRODUCTION

The majority of the well-known inhibitors [1-9] for metal corrosion protection are organic compounds containing electronegative atoms [10-18] (such as, N, S, P, O, etc.), the unsaturated bonds (such as, double bonds or triple bonds, etc.) and the plane conjugated systems including all kinds of aromatic cycles [19-29] which allow an adsorption [30-33] on the metal surface [34-42]. It has been observed that the adsorption of these inhibitors depends on the physico-chemical properties of the functional groups and the electron density at the donor atom. The adsorption occurs due to the interaction of the lone pair and/ or π -orbital's of inhibitor with d-orbital's of the metal surface atoms, which evokes a greater adsorption of the inhibitor molecules onto the surface, leading to the formation of a corrosion protection film [43-45]. Furthermore, adsorption is also influenced by the structure and the charge of metal surface, and the type of testing electrolyte [46]. The choice of effective inhibitors is based on their mechanism of action and electron-donating ability. The significant criteria involved in this selection are molecular structure, electron density on the donor atoms, solubility and dispensability [47-50]. Schiff base, an organic compound having general formula $R-C=N-R'$ where R and R' are aryl, alkyl or cycloalkyl or heterocyclic groups formed by the condensation of an amine and a carbonyl group, is a potential inhibitor. The greatest advantage of many Schiff base compounds is that they can be conveniently and easily synthesized from relatively cheap material. Schiff base compounds due to the presence of the $-C=N-$ group, electronegative nitrogen, sulfur and/or oxygen atoms in the molecule, have been reported to be effective inhibitors for the corrosion of iron and steel in acidic and alkaline media by several authors [51-71]. The presence of $-C=N-$ group in Schiff base molecules enhances their adsorption ability and corrosion inhibition efficiency [21, 72]. In addition, the planarity (π) and lone pair of electrons present on the N atoms are the important structural features that determine the adsorption of these molecules to the metal surface [73]. Adsorption of inhibitors on the metal surface involves formation of two types of interaction (physical adsorption and chemical adsorption). Physical adsorption requires the presence of both electrically charged surface of the metal and charged species in the bulk solution. The second one, chemisorptions process involves charge sharing or charge transfer from the inhibitor molecules to the metal surface to form a coordinate type bond and takes place in the presence of heteroatom's (P, N, S, O, etc.) with lone pairs of electrons and/or aromatic ring in the molecular structure [46,68,74-85]. In any case, adsorption is general over the metal surface and the resulting adsorption layer function as a barrier, isolating the metal from the corrosion [16]. The inhibition efficiency has found to be closely related to inhibitor adsorption abilities and molecular properties for different kinds of organic compounds [86-88]. The efficiency of an inhibitor does not only depend on its structure, but also on the characteristics of the environment in which it acts; the nature of the metal and other experimental conditions. Under certain conditions, the electronic structure of the organic inhibitors has a key influence on the corrosion inhibition efficiency to the metal. The choice of effective inhibitors has been mostly done by using the empirical knowledge based on their macroscopically physicochemical properties, mechanism of action and electron donating ability [89,90]. The most significant criteria involved in the selection of an inhibitor are its hydrophobicity, molecular structure, electron density at their donor atoms, solubility and dispersibility. Theoretical chemistry has been used recently to explain the mechanism of corrosion inhibition, such as quantum chemical calculations [88, 90-93]. Quantum chemical calculations have been proved to be a very powerful tool for studying the mechanism [94-96]. The development of semi-empirical quantum chemical calculations emphasizes the scientific approaches involved in the selection of inhibitors by correlating the experimental data with quantum-chemical properties. The highest occupied molecular orbital (HOMO), lowest unoccupied molecular orbital (LUMO), charges on reactive centre, dipole moment (μ) and conformations of molecules have been used to achieve the appropriate correlations [95, 97-101]. In continuation of our earlier work on Schiff base derivatives [102], we have investigated the corrosion behaviour of iron in acidic and alkaline media (2.0 M HNO_3 and 2.0 M NaOH) in the presence of (PSCs) using chemical and electrochemical techniques.

The objective of this work is to present a theoretical study on electronic and molecular structures of neutral and cationic (diprotonated) forms of (PSCs) and to determine relationship between molecular structure of the compounds and inhibition efficiency. The structural parameters, such as the frontier molecular orbital energy HOMO, LUMO, the charge distribution of the studied inhibitors, the absolute electronegativity (χ) values, dipole moment (μ), total energy (E_{total}), hardness (η) and the fraction of electrons (ΔN) transfer from inhibitors to iron were calculated and correlated with inhibition efficiencies (% IE).

EXPERIMENTAL METHOD

Synthesize of Schiff bases

The used Schiff base compounds were synthesized from 1:1 mol ratios of amine with the optimum salicylaldehyde and/or benzaldehyde through a condensation reaction in ethanoic media in a reflux condenser for 4hrs. The solution

was further concentrated, cooled in ice bath and the compound formed. The products were recrystallized twice from ethanol, washed by water and dried under vacuum to afford pale yellow crystals [102,103]. The molecular structure of the synthesized Schiff base was determined by chemical analyses for the atoms, IR, UV-Visible spectroscopic investigation; and mass spectroscopy techniques and is given in **Figure 1**. The corrosion tests were performed in aerated 2.0 M HNO₃ and 2.0 M NaOH solutions in with and without various (PSCs) concentrations. The Schiff bases containing nitrogen and oxygen as hetero atom; Schiff base **1** = 4-(2-Hydroxy naphthylidene amino) antipyrine, Schiff base **2** = 4-(2-Hydroxybenzylidene amino) antipyrine, Schiff base **3** = 3-(2-Hydroxynaphthylideneamino)-1,2,4-triazole, Schiff base **4** = 3-(2-Hydroxybenzylideneamino)-1,2,4-triazole, Schiff base **5** = 3-(4-Hydroxy benzylidene amino)-1,2,4-triazole ; were synthesized and characterized by ¹H NMR, IR spectroscopy and element analysis before use [104,105]. For each experiment, a freshly prepared solution was used. The test solutions were opened to the atmosphere, and the temperature was controlled thermostatically at 303 K.

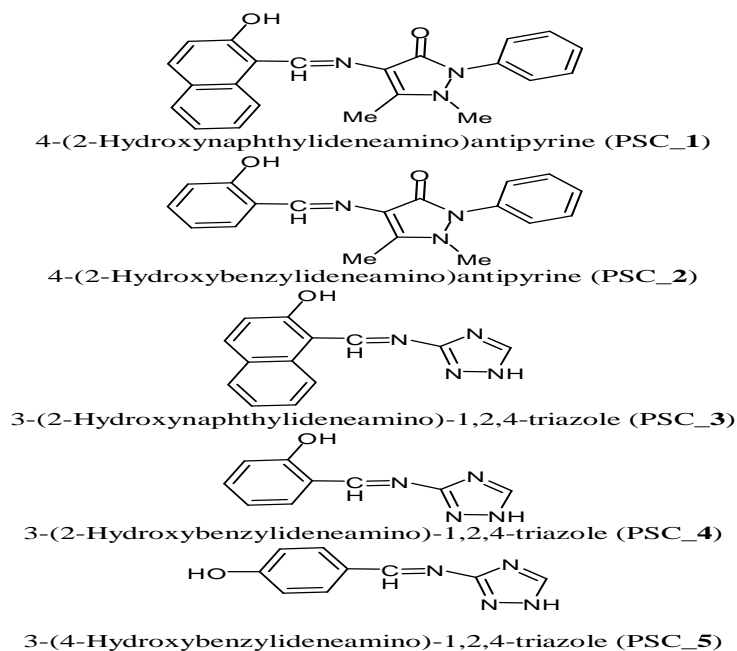


Figure 1. Structural formulae of polydentate Schiff base compound (PSCs)

Electrodes and electrolytes

The corrosion tests were performed on a freshly prepared sheet of iron specimen with a chemical composition (in wt. %): (0.16% C, 0.05% Si, 0.37% Mn, 0.015% S) and Fe balance. The test specimens used in the weight loss experiment were mechanically cut into 2.0 cm x 2.0 cm x 0.1cm sizes, then abraded with SiC abrasive papers 320, 400 and 600 grit, respectively, washed in absolute ethanol and acetone, dried in room temperature and stored in a moisture free desiccators before their use in corrosion studies [31,32]. For the weight loss measurements, a 2mm diameter small hole was drilled near the upper edge of the specimen to accommodate a suspension hook. For electrochemical study, specimens was soldered with Cu-wire for electrical connection and mounted into the epoxy resin to offer only one active flat surface exposed to the corrosive environment. Before each experiment, the electrode was first mechanically abraded with a sequence of emery papers of different grades (400, 800, 1000 and 1200), followed by washing with double distilled water and finally degreased with acetone and dried at room temperature. The corrosive solutions (2.0 M HNO₃ and 2.0 M NaOH) were prepared by dilution of analar analytical grade with double distilled water without further purification. The concentration range of employed inhibitors was 5.0×10^{-7} to 1.0×10^{-4} M in acidic and alkaline media.

Measurements

Three experimental methods weight loss, thermometric and electrochemical polarization curves were applied in my previous work [102] and the practical corrosion inhibition efficiencies (% IE) of the investigated Schiff bases (PSCs) were determined.

Gravimetric measurements

The gravimetric method (weight loss) is probably the most widely used method of inhibition assessment [106–109]. The simplicity and reliability of the measurement offered by the weight loss method is such that the technique forms the baseline method of measurement in many corrosion monitoring programmes [110]. Weight loss measurements were conducted under total immersion using 250 mL capacity beakers containing 100 mL test solution at 303 K maintained in a thermostatic water bath. The iron coupons were weighed and suspended in the beaker with the help of rod and hook. The coupons were retrieved at 0.5 h interval progressively for 6 h, washed thoroughly in 20%

NaOH solution containing 200 g/l of zinc dust [45] with bristle brush, rinsed severally in deionized water, cleaned, dried in acetone, and re-weighed. The weight loss, in grams, was taken as the difference in the weight of the iron coupons before and after immersion in different test solutions. In order to get good reproducibility, experiments were carried out in triplicate. In this present study, the standard deviation values among parallel triplicate experiments were found to be smaller than 5%, indicating good reproducibility. The corrosion rate (W) was calculated from the following equation [54,111,112]:

$$W = \frac{m_1 - m_2}{S \cdot t} \quad (1)$$

Where m_1 is the mass of the iron coupon before immersion in (mg), m_2 the mass of the iron coupon after immersion in (mg), S is the total area of the iron coupon (cm^2), t is the corrosion time in (h) and W is the corrosion rate in ($\text{mg cm}^{-2} \text{h}^{-1}$). With the corrosion rate, the percentage inhibition efficiency (% IE) was calculated using the following equation [113,114]:

$$\% \text{ IE} = \frac{W_0 - W}{W_0} \quad (2)$$

Where W_0 and W are the values of corrosion rates of iron in uninhibited and inhibited solutions, respectively.

Spectrophotometric measurements

UV–Visible absorption spectrophotometric method was carried out on the prepared iron samples after immersion in aerated 2.0 M HNO_3 and/or 2.0 M NaOH with and without addition of concentration 10^{-4} M of: PSC_1, PSC_2 and PSC_5 at 303 K for 3 days. All the spectra measurements were carried out using a Perkin-Elmer UV–Visible Lambda 2 spectrophotometer.

Thermometric measurements

The reaction vessel used was basically the same as that described by Mylius [115]. An iron piece (1 x 10 x 0.1 cm) was immersed in 30 cm^3 of either 2.0 M HNO_3 or 2.0 M NaOH in the absence and presence of additives, and the temperature of the system was followed as a function of time. The procedure for the determination of the metal dissolution rate by the thermometric method has been described previously [115, 116]. The reaction number (RN) is defined [117] as:

$$RN = \frac{(T_{max} - T_i)}{t} \quad (3)$$

where T_{max} and T_i , are the maximum and initial temperatures, respectively, and t is the time (in minutes) required to reach the maximum temperature. The percent reduction in RN [118] is then given as:

$$\% \text{ reduction in RN} = \frac{(RN_{free} - RN_{inh})}{RN_{free}} \times 100 \quad (4)$$

Electrochemical measurements

Electrochemical experiments were carried out using a standard electrochemical three-electrode cell. Iron acts as working electrode (WE), saturated calomel electrode (SCE). As reference electrode and platinum was used as counter electrode. Polarization measurements were carried out using a (Wenking Potentiostan model POS 73). Potentials and currents were determined by digital multi meters. Corrosion current densities (i_{corr}) were determined by extrapolation of the anodic and cathodic Tafel lines to the free corrosion potential value (E_{corr}). The inhibition efficiencies at different

inhibitor concentrations were calculated using the following equation:

$$\% \text{ IE} = \frac{I_{\text{corr}} - I_{\text{inh, corr}}}{I_{\text{corr}}} \times 100 \quad (5)$$

Where I_{corr} and $I_{\text{inh, corr}}$ are the corrosion current density in the absence and presence of an inhibitor, respectively [119].

Theory and computational details

DFT (density functional theory) methods were used in this study. These methods have become very popular in recent years because they can reach exactitude similar to other methods in less time and less expensive from the computational point of view. In agreement with the DFT results, energy of the fundamental state of a polyelectronic system can be expressed through the total electronic density, and in fact, the use of electronic density instead of wave function for calculating the energy constitutes the fundamental base of DFT [96]. The initial geometry optimizations and frequency calculations were done at the Hartree–Fock (HF) level of theory using the standard 6-31G* basis set which requests that a set of d function be included for each atom heavier and P function for hydrogen. The HF geometry was later reoptimized using density functional theory (DFT) with frequency calculation using 6-31G** basis set. The frequency calculation were carried out to confirm form a minimum local studied structures. The calculations were done using the Becke's Three Parameter Hybrid Method (B3) [120] employing the correlation functional of Lee, Yang and Parr (LYP) [121]; including both local and non-local terms. All calculations are performed by using the Gaussian 09W program [122]. Single point calculations were carried for the optimized structures using B3LYP/6-311++G** level of theory. The natural bonding orbital's (NBO) calculations [123] were performed using NBO 3.1 program as implemented in the Gaussian 03 package at the DFT/B3LYP/6-311G(d, p) level in order to explore the charge distribution for the studied compounds.

RESULTS AND DISCUSSION

Quantum chemical studies

The density functional theory (DFT) is one of the most important theoretical models used in explaining the science of solids and chemistry. A number of chemical concepts have been correlated within the framework of DFT [124]. The most fundamental parameter in DFT is the electron density $\rho(r)$ upon which all the chemical quantities are expressed [125]. The structural parameters calculated through the $\rho(r)$ concept, compare well with the parameters calculated by the ψ concept [126]. Since the theory is simpler than quantum mechanics, the interest has grown in understanding the structure, properties, reactivity, and dynamics of atoms, molecules and clusters using DFT. In the field of reaction chemistry, DFT exceeds the limit of wave mechanics [127], and it is emerging as a unique approach for the study of reaction mechanism [128]. Thus, charge-based parameters have been widely employed as chemical reactivity indices or as measures of weak intermolecular interactions. Despite its usefulness, the concept of a partial atomic charge is somewhat arbitrary, because it depends on the method used to delimit between one atom and the next. As a consequence, there are many methods for estimating the partial charges. Mulliken population analysis [129,130] is mostly used for the calculation of the charge distribution in a molecule. These numerical quantities are easy to obtain and they provide at least a qualitative understanding of the structure and reactivity of molecules [131]. Furthermore, atomic charges are used for the description of the molecular polarity of molecules. Frontier orbital theory is useful in predicting adsorption centers of the inhibitor molecules responsible for the inter-action with surface metal atoms [95,132]. Terms involving the frontier MO could provide dominative contribution, because of the inverse dependence of stabilization energy on orbital energy difference [132]. Moreover, the gap between the HOMO and LUMO energy levels of the molecules was another important factor that should be considered. Reportedly, excellent corrosion inhibitors are usually those organic compounds who not only offer electrons to unoccupied orbital of the metal, but also accept free electrons from the metal [92,132]. Recently, the density functional theory (DFT) has been used to analyze the characteristics of the inhibitor/surface mechanism and to describe the structural nature of the inhibitor on the corrosion process [133–135]. Furthermore, DFT is considered a very useful technique to probe the inhibitor/surface interaction as well as to analyze the experimental data. Thus in the present investigation, quantum chemical calculation using DFT was employed to explain, correlate, confirm and finally support the experimental results obtained in my previous [102] study, and to further give insight into the inhibition action of PSCs on the iron surface. For the purpose of determining the active sites of the inhibitor molecule, three influence factors: natural atomic charge, distribution of frontier orbital, and

Fukui indices are considered. According to classical chemical theory, all chemical interactions are by either electrostatic or orbital. Electrical charges in the molecule were obviously the driving force of electrostatic interactions it has been proven that local electron densities or charges are important in many chemical reactions and physico-chemical properties of compound [136]. Highest occupied molecular orbital energy (E_{HOMO}) and lowest unoccupied molecular orbital energy (E_{LUMO}) are very popular quantum chemical parameters. These orbitals, also called the frontier orbitals, determine the way the molecule interacts with other species. The HOMO is the orbital that could act as an electron donor, since it is the outermost (highest energy) orbital containing electrons. The LUMO is the orbital that could act as the electron acceptor, since it is the innermost (lowest energy) orbital that has room to accept electrons. According to the frontier molecular orbital theory, the formation of a transition state is due to an interaction between the frontier orbitals (HOMO and LUMO) of reactants [137]. The energy of the HOMO is directly related to the ionization potential and the energy of the LUMO is directly related to the electron affinity. The HOMO–LUMO gap, i.e. the difference in energy between the HOMO and LUMO, is an important stability index [138]. A large HOMO–LUMO gap implies high stability for the molecule in chemical reactions [139]. The concept of “activation hardness” has been also defined on the basis of the HOMO–LUMO energy gap. The qualitative definition of hardness is closely related to the polarizability, since a decrease of the energy gap usually leads to easier polarization of the molecule [140]. Table 1 presents the calculated energy levels of the HOMO and LUMO for the five selected compounds. The measured average inhibition efficiencies (% IE) of these five PSCs were also listed in the table (these data were measured in 2.0 M HNO_3 acid and 2.0M NaOH solutions at 303 K [102]. According to Emregu'l [71], when length of aminic nitrogen-containing carbon bone chain increased, the corrosion inhibition efficiency increased significantly. The quantum chemistry calculation in this study revealed that as the length increases, the HOMO energy level boosted significantly while the energy gap dropped sharply. The linear correlation between MO energy level and the corrosion inhibition efficiency of the PSCs (Figures 2–4) proved that the higher the HOMO energy of the inhibitor, the greater the trend of offering electrons to unoccupied d orbital of the metal, and the higher the corrosion inhibition efficiency for iron in HNO_3 acid and NaOH solutions; in addition, the lower the LUMO energy, the easier the acceptance of electrons from metal surface, as the HOMO – LUMO energy gap decreased and the efficiency of inhibitor improved. The relationship between corrosion inhibition efficiency and HOMO energy levels for these five PSCs is plotted in Figure 2. As clearly seen in the figure, the inhibition efficiency increased with the E_{HOMO} level rising. In Figure 3, inhibition efficiency is plotted against the LUMO energy, showing the inhibition efficiency reduced with the E_{LUMO} level increase. The relationship between the inhibition efficiency and the energy gap ($E_{\text{LUMO}} - E_{\text{HOMO}}$) is negative as shown in Figure 4. The total energy (E_{total}), calculated by quantum chemical methods is also a beneficial parameter. The total energy of a system were presented in Figure 5, is composed of the internal, potential, and kinetic energy. Hohenberg and Kohn [141] proved that the total energy of a system including that of the many body effects of electrons (exchange and correlation) in the presence of static external potential (for example, the atomic nuclei) is a unique functional of the charge density. The minimum value of the total energy functional is the ground state energy of the system. The electronic charge density which yields this minimum is then the exact single particle ground state energy. The most widely used quantity to describe the polarity is the dipole moment (μ) of the molecule [142]. Dipole moment (μ) is the measure of polarity of a polar covalent bond. It is defined as the product of charge on the atoms and the distance between the two bonded atoms. The total dipole moment, however, reflects only the global polarity of a molecule. For a complete molecule the total molecular dipole moment may be approximated as the vector sum of individual bond dipole moments (Figure 6). Figures 7-10 show the optimized geometry, the HOMO density distribution, the LUMO density distribution and the Mullikan charge population analysis plots for PSCs molecules obtained with DFT at the B3LYP/6-311++G** level of theory. The reactive ability of the inhibitor is considered to be closely related to their frontier molecular orbitals, the HOMO and LUMO. The frontier molecule orbital density distributions of five PSCs were presented in Figures 7, 8. As seen from the figures, the populations the HOMO focused around the carbon chain containing aminic nitrogen. But the LUMO densities were mainly around the benzene cyclic. Higher HOMO energy (E_{HOMO}) of the molecule means a higher electron-donating ability to appropriate acceptor molecules with low-energy empty molecular orbital and thus explains the adsorption on metallic surfaces by way of delocalized pairs of π -electrons. E_{LUMO} , the energy of the lowest unoccupied molecular orbital signifies the electron receiving tendency of a molecule. The Mulliken charge populations of the five PSCs were also presented in Figure 9. It can see that the area of carbon bone chain containing aminic nitrogen, hydroxyl, and methyl, charged a large electron density and might form adsorption active centers. Accordingly, the difference between E_{LUMO} and E_{HOMO} energy levels ($\Delta E = E_{\text{LUMO}} - E_{\text{HOMO}}$) and the dipole moment (μ) were also determined. The global hardness (η) is approximated as $\Delta E/2$, and can be defined under the principle of chemical hardness and softness [143]. These parameters also provide information about the reactive behavior of molecules and are presented in Table 1. These theoretical parameters were calculated in the gas phase, aqueous phase as well as in the protonated form of PSCs. The calculated parameters in gas phase as well as in the presence of a solvent did not exhibit important differences. From Figures 7 and 8, it could be seen that PSCs have similar HOMO and LUMO distributions, which were all located on the entire PSCs moiety. This is

due to the presence of nitrogen and oxygen atoms together with several π -electrons on the entire molecule. Thus, unoccupied d-orbital of Fe atom can accept electrons from inhibitor molecule to form coordinate bond. Also the inhibitor molecule can accept electrons from Fe atom with its anti-bonding orbital's to form back-donating bond. Figure 10. Shows B3LYP/6-311G** selected bond length for the optimized geometry of the studied (PSCs) compounds calculated for PSCs. It has been reported that the more negative the atomic charges of the adsorbed centre, the more easily the atom donates its electron to the unoccupied orbital of the metal [143]. It is clear from Figure 10, that nitrogen and oxygen as well as some carbons atoms carries negative charge centers which could offer electrons to the iron surface to form a coordinate bond. This shows that the two N and O atoms are the probable reactive sites for the adsorption of iron. Higher values of E_{HOMO} are likely to indicate a tendency of the molecule to donate electrons to appropriate acceptor molecules with low energy or empty electron orbital. It is evident from Table 1 that PSCs has the highest E_{HOMO} in the gas and aqueous phase and a lower E_{HOMO} in the protonated form. This means that the electron-donating ability of PSCs is weaker in the protonated form. This confirms the experimental results that interaction between PSCs and iron is electrostatic in nature (physisorption). The energy of the LUMO is directly related to the electron affinity and characterizes the susceptibility of the molecule towards attack by neuclophiles. The lower the values of E_{LUMO} are, the stronger the electron accepting abilities of molecules. It is clear that the protonated form of PSCs exhibits the lowest E_{HOMO} , making the protonated form the most likely form for the interaction of iron with PSCs molecule. Low values of the energy gap (ΔE) will provide good inhibition efficiencies, because the excitation energy to remove an electron from the last occupied orbital will be low [144]. A molecule with a low energy gap is more polarizable and is generally associated with a high chemical reactivity, low kinetic stability and is termed soft molecule [145]. The numbers of transferred electrons (ΔN) depending on the quantum chemical method [146,147].

Table 1. Molecular property of (PSCs) calculated with B3LYP/6-311++G** level of Theory

Inhibitor (PSCs)	$E_{\text{HOMO}}(\text{eV})$	$E_{\text{LUMO}}(\text{eV})$	$\Delta E_{\text{gap}}=(E_{\text{LUMO}}(\text{eV}) - E_{\text{HOMO}}(\text{eV}))$	Hardness (η)	Total energy(a.u.)	Dipole moment (Debye)	(% IE) ^a	
							HNO ₃	NaOH
1	-5.912	-1.831	4.082	2.041	-1165.9688	3.444	78.4	58.3
2	-6.148	-1.118	5.021	2.510	-1012.2904	6.790	76.1	55.3
3	-6.305	-2.533	3.772	1.886	-795.82109	7.677	75.2	54.1
4	-6.755	-2.062	4.693	2.346	-642.12133	8.641	74.1	52.7
5	-6.457	-2.007	4.449	2.224	-642.13614	1.909	73.1	48.2

All the experimental tests were carried out at the inhibitor concentration of 0.1mM, from Ref. [102].

^aMeasured by weight loss method.

Table 2. Effect of 4-(2-hydroxynaphthylidene amino) antipyrine(PSC_1)concentration on the thermometric parameters for iron in 2M HNO₃acid

Conc. mol/L	Ti C°	T max. C°	T min.	Δt min.	Log t min.	Θ	R N C° min ⁻¹	% red. in RN
0.0	19.5	50.8	68	--	--	--	0.460	--
5x10 ⁻⁷	17.8	46.8	130	62	1.792	0.515	0.223	51.6
1x10 ⁻⁶	17.5	46.5	141	73	1.863	0.554	0.205	55.4
5x10 ⁻⁶	17.0	45.7	155	87	1.939	0.597	0.185	59.8
1x10 ⁻⁵	18.0	44.1	177	109	2.037	0.680	0.147	68.0
5x10 ⁻⁵	18.0	44.0	190	122	2.086	0.702	0.136	70.3
1x10 ⁻⁴	18.0	41.0	200	132	2.120	0.750	0.115	75.9

Table 3. Comparison between percent corrosion inhibition efficiency (% IE) of (PSC_1-5), as determined by weight - loss, thermometric and polarization at 1x10⁻⁴ M concentration at 303 K

Inhibitor	% Inhibition					
	Weight-loss		Thermometric		Polarization	
	HNO ₃	NaOH	HNO ₃	NaOH	HNO ₃	NaOH
PSC_1	78.4	58.3	75.9	--	73.8	63.2
PSC_2	76.1	55.3	75.0	--	72.0	58.1
PSC_3	75.2	54.1	74.1	--	71.1	62.3
PSC_4	74.1	52.7	73.7	--	69.8	56.8
PSC_5	73.1	48.2	71.5	--	68.6	55.3

Table 4. Curve fitting data to the kinetic-thermodynamic model ($r = 0.94$) and the Temkin adsorption isotherm for (PSC_1-5) in 2.0 M HNO₃ and 2.0 M NaOH media at 303 K

Inhibitor	Medium	Kinetic model			Temkin adsorption isotherm		
		1/y	K _b	-ΔG° kJ/mol	-f	K _{ads}	-ΔG° kJ/mol
PSC_1	HNO ₃	10.44	1.8x10 ⁸	37.75	23.46	36307	16.33
	NaOH	4.80	3.3x10 ⁴	16.01	31.55	13803	13.89
PSC_2	HNO ₃	10.00	1.2x10 ⁸	36.81	24.16	31622	15.98
	NaOH	4.54	2.2x10 ⁴	15.11	33.30	12302	13.60
PSC_3	HNO ₃	9.32	7.3x10 ⁷	35.50	24.44	30408	15.88
	NaOH	4.16	1.8x10 ⁴	14.53	33.97	11800	13.50
PSC_4	HNO ₃	7.98	5.3x10 ⁷	34.67	24.82	28575	15.75
	NaOH	3.85	9.7x10 ³	13.01	34.47	9332	12.91
PSC_5	HNO ₃	6.73	4.2x10 ⁷	34.18	25.15	27227	15.60
	NaOH	3.72	8.6x10 ³	12.71	37.86	8917	12.30

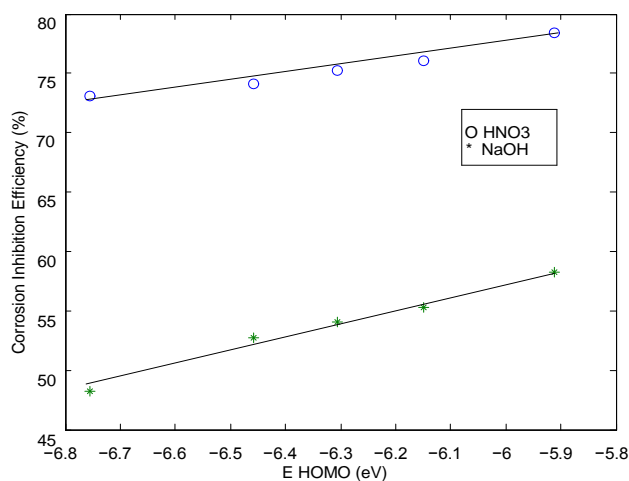


Figure 2. Correlation of HOMO energy with percent inhibition efficiency of PSCs

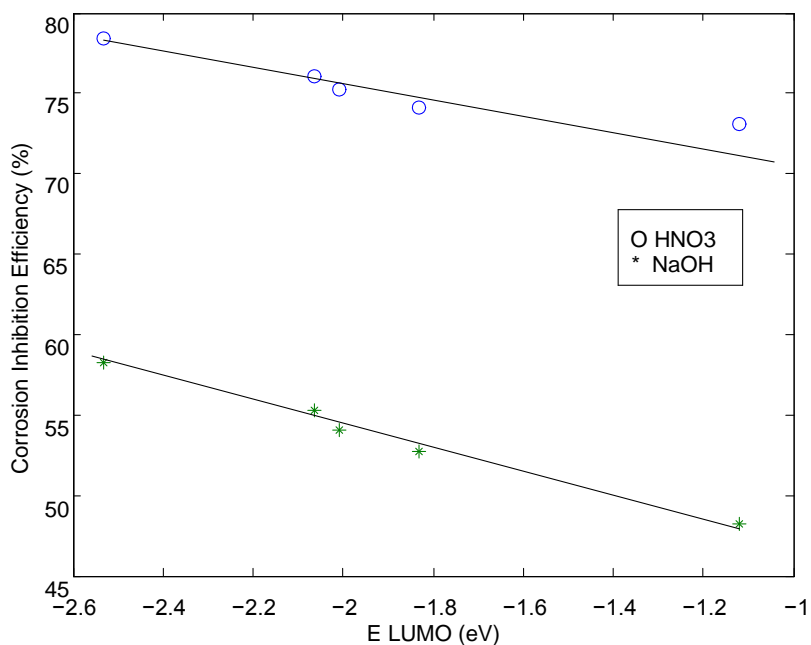


Figure 3. Correlation of LUMO energy with percent inhibition efficiency of PSCs

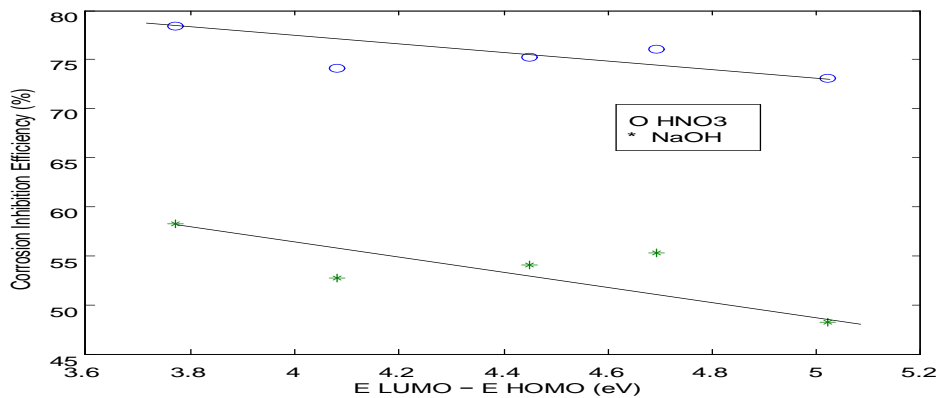


Figure 4. Correlation of LUMO - HOMO energy gaps with percent inhibition efficiency of PSCs

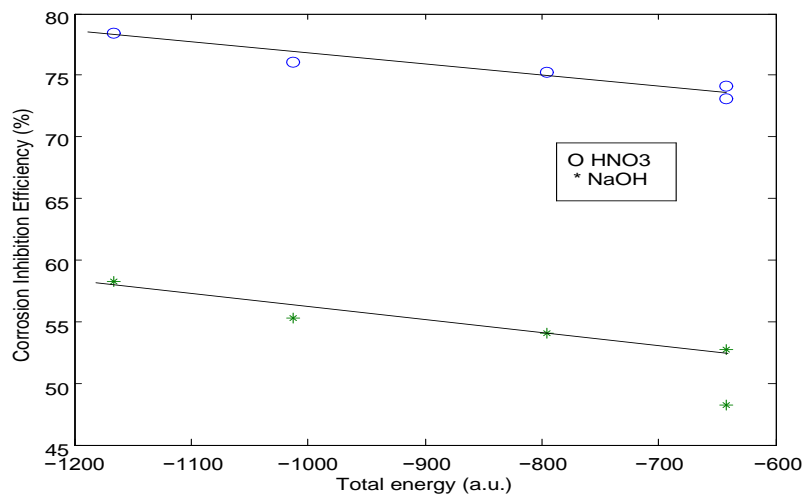


Figure 5. Correlation of Total energy with percent inhibition efficiency of PSCs

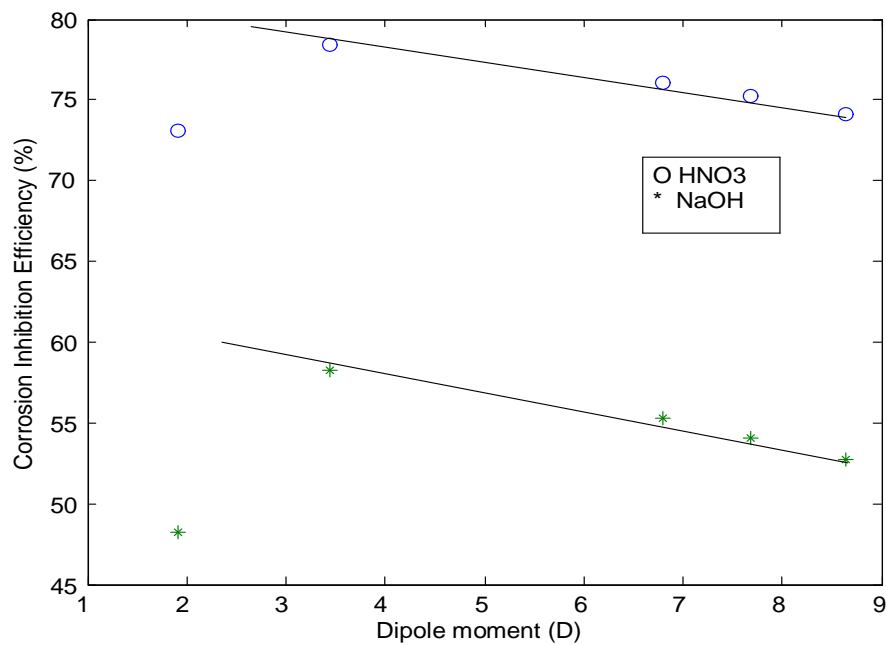


Figure 6. Correlation of dipole moment with percent inhibition efficiency of PSCs

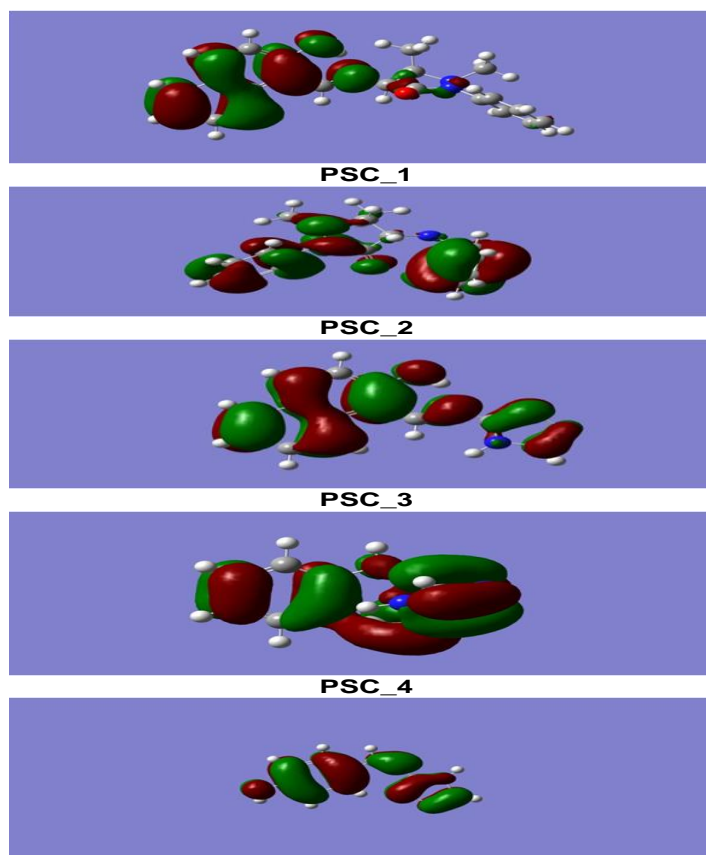


Figure 7. The highest occupied molecular orbital (HOMO) density of (PSCs) using DFT at the B3LYP/6-311++G** level

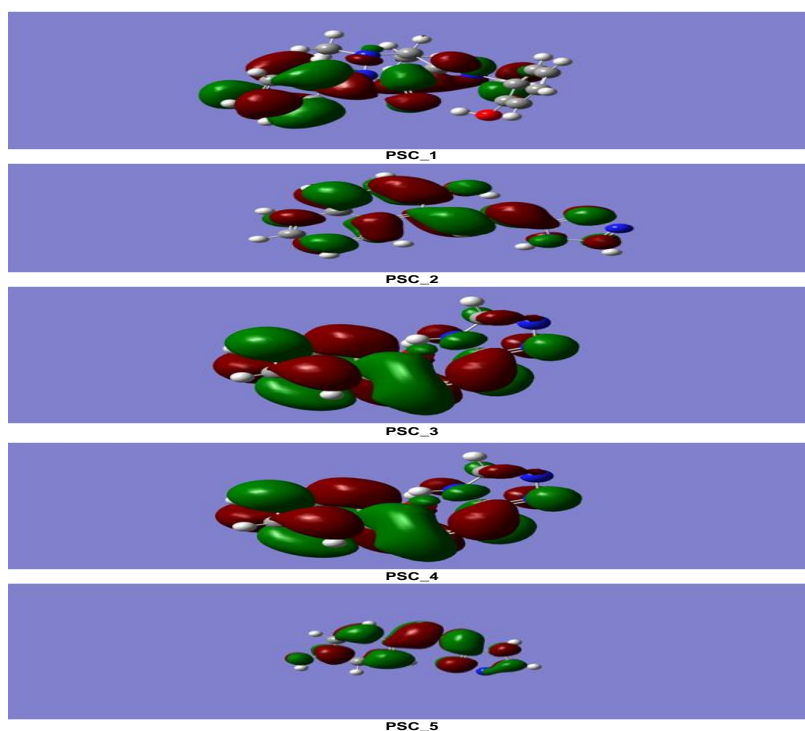
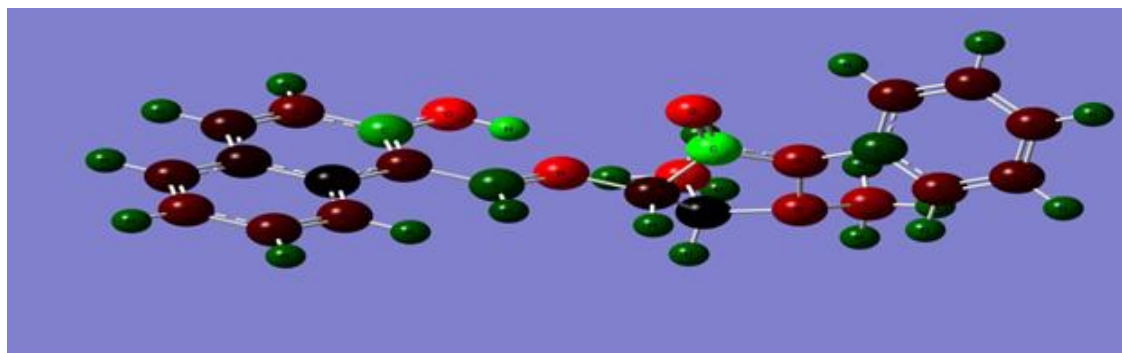
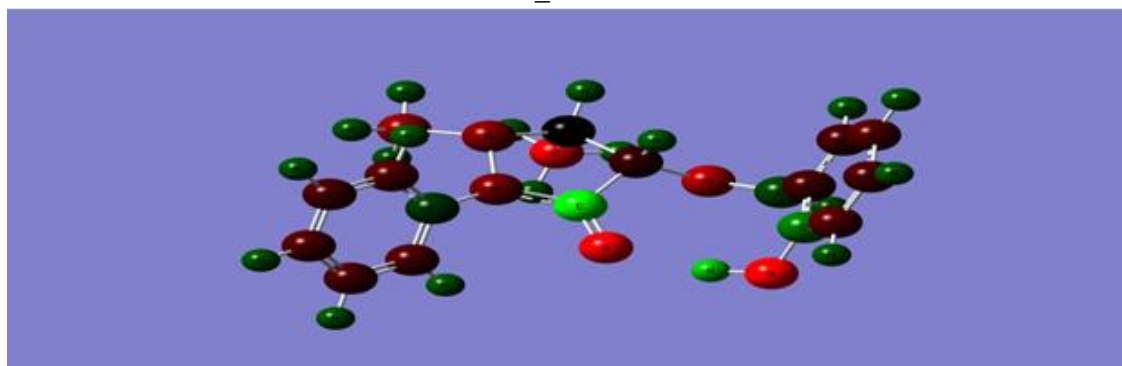


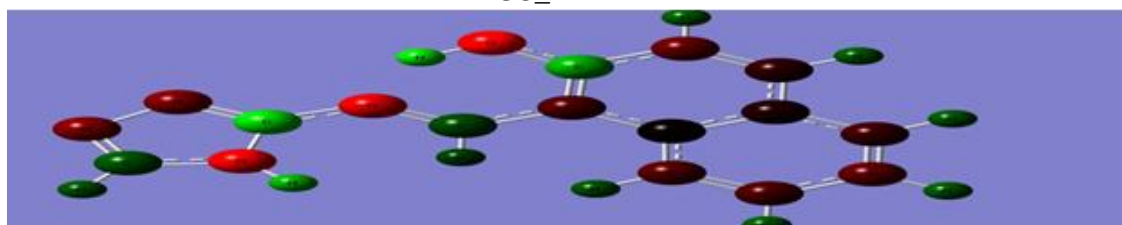
Figure 8. The lowest unoccupied molecular orbital (LUMO) density of (PSCs) using DFT at the B3LYP/6-311++G** level



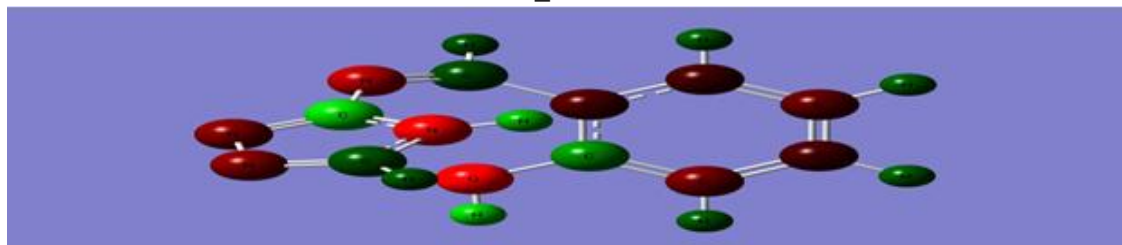
PSC_1



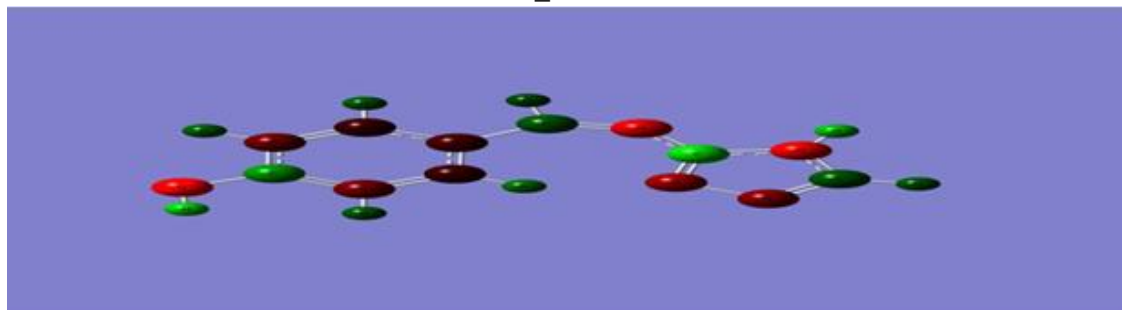
PSC_2



PSC_3



PSC_4



PSC_5

Figure 9. The natural bond orbital's charge population of the studied PSCs compounds

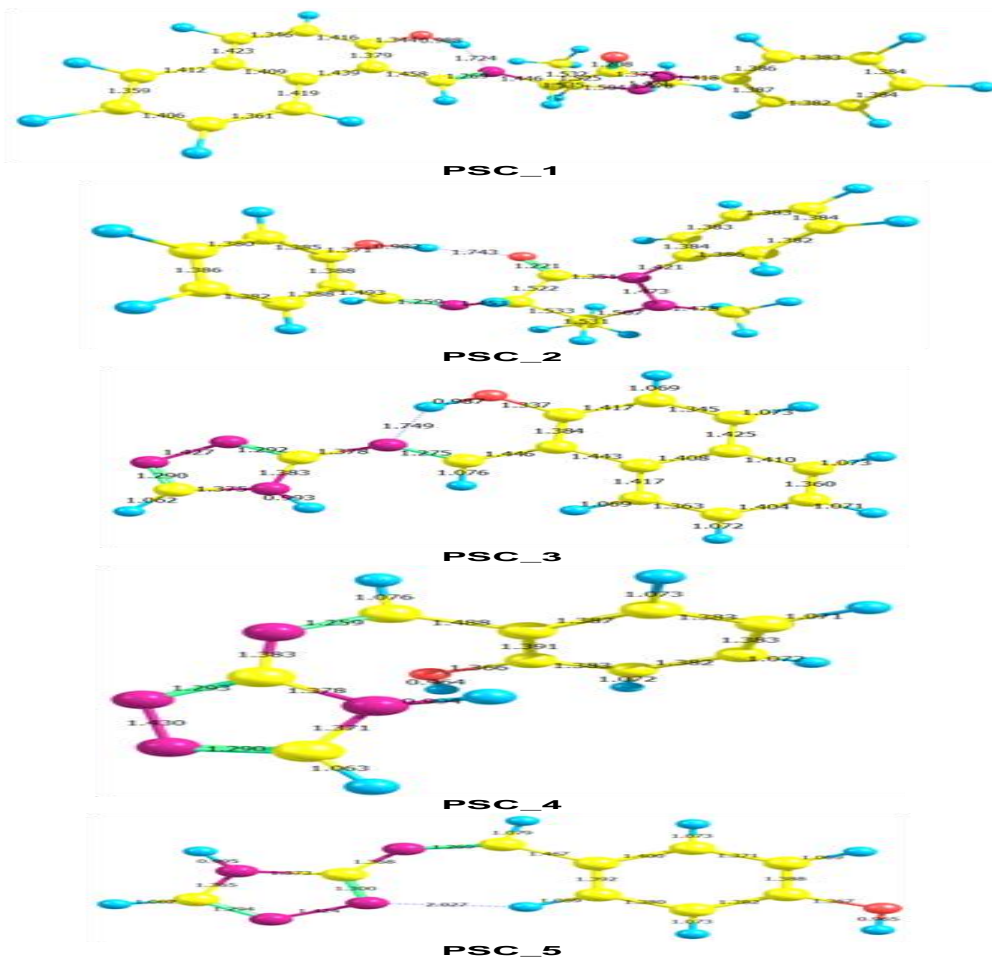


Figure 10. B3LYP/6-311G**selected bond length for the optimized geometry of the studied (PSCs) compounds. Bond length in angstrom

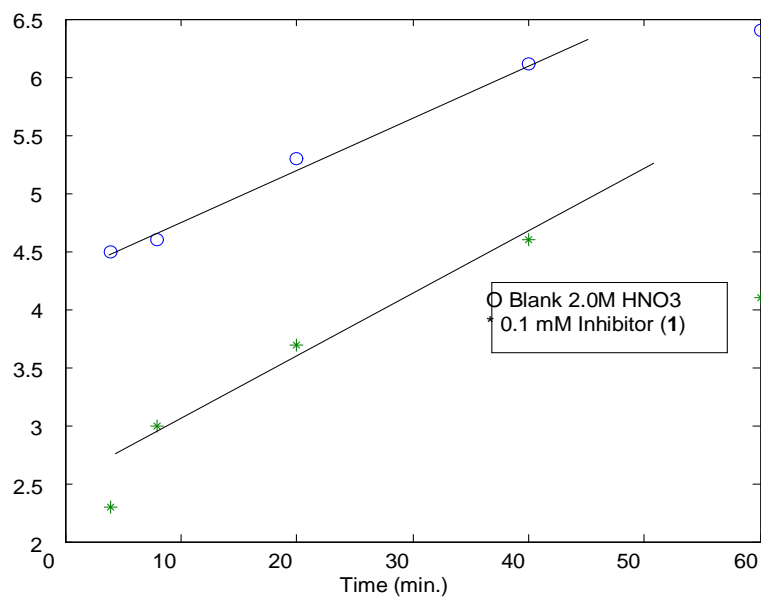


Figure 11. The plot of $\ln Wt$ against t for iron corrosion in 2.0 M HNO_3 with and without inhibitor (PSC₁)

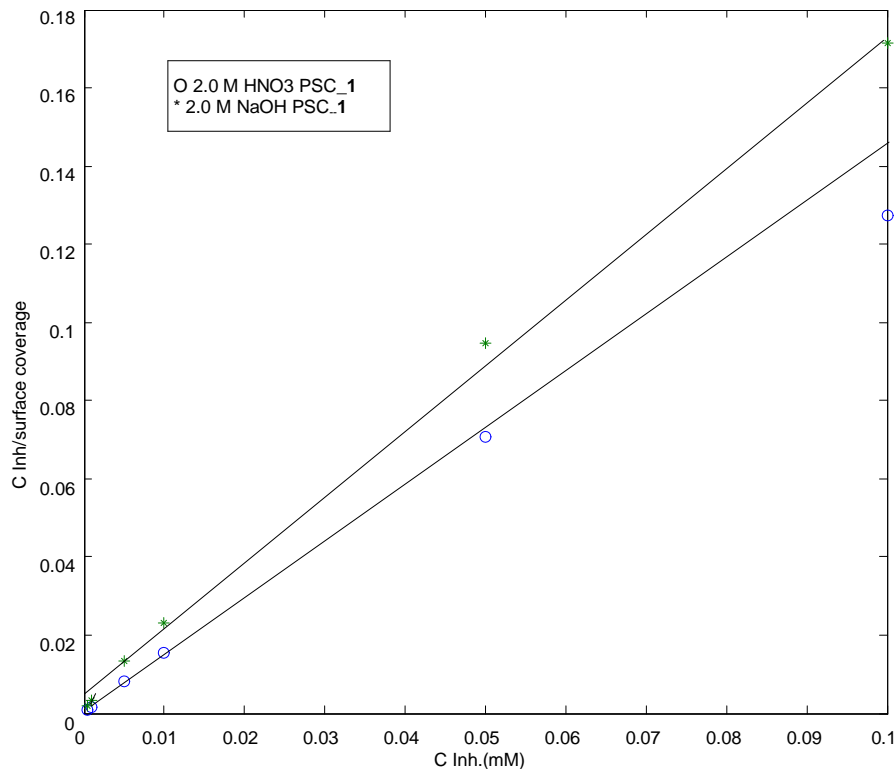


Figure 12. Relation between C Inh. and C Inh./surface coverage of (PSC --1). for iron in HNO3 and NaOH at 303 K

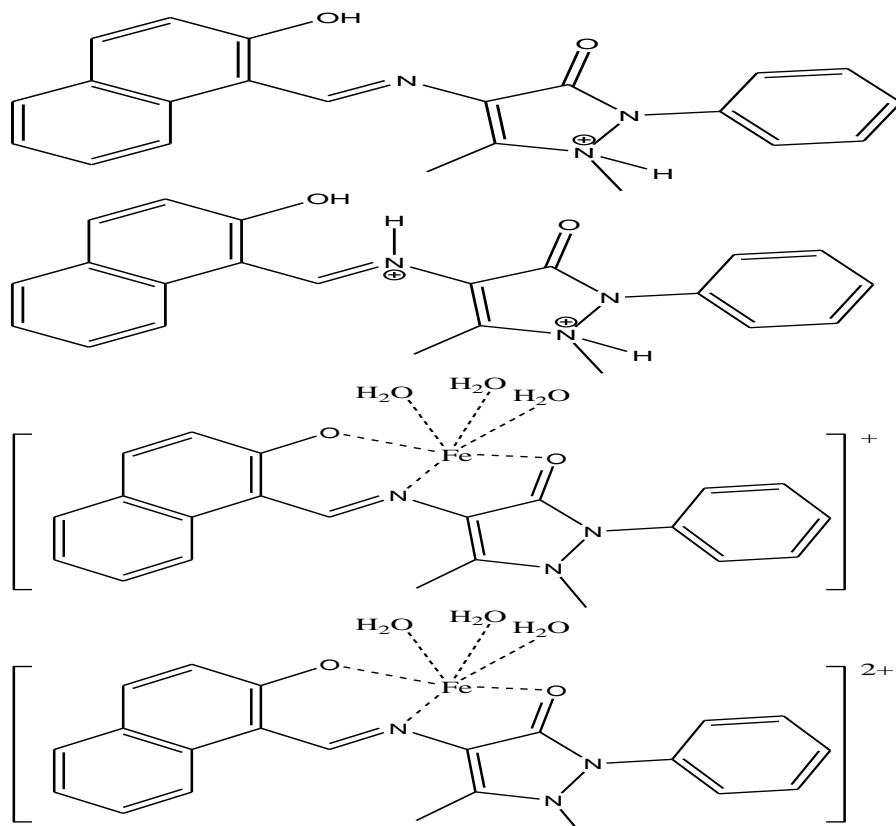


Figure 13. Proposed structure of the complex compounds formed between PSC_1 and Fe²⁺

$$\Delta N = (\chi_{\text{Fe}} - \chi_{\text{inh}}) / [2(\eta_{\text{Fe}} + \eta_{\text{inh}})] \quad (6)$$

Where χ_{Fe} and χ_{inh} denote the absolute electro negativity of iron and the inhibitor molecule, respectively; χ_{Fe} and χ_{inh} denote the absolute hardness of iron and the inhibitor molecule, respectively. These quantities are related to electron affinity (A) and ionization potential (I)

$$\chi = \frac{I + A}{2} \quad (7)$$

$$\eta = \frac{I - A}{2} \quad (8)$$

I and A are related in turn to E_{HOMO} and E_{LUMO} , by the following relation [148]: $I = E_{\text{HOMO}}$ (9)

$$A = -E_{\text{LUMO}} \quad (10)$$

Values of χ and η were calculated by using the values of I and A obtained from quantum chemical calculation. Using a theoretical χ value of 7eV/mol and η value of 0 eV/mol for iron atom [146]. The inhibition efficiency increased with the ΔN increase. According to other reports [146,147], values of ΔN showed inhibition effect resulted from electrons donation. Agreeing with Lukovits's study [112], the inhibition efficiency increased with increasing electron-donating ability at the metal surface. In this study, the five PSCs were the donators of electrons, and the iron surface was the acceptor. The compounds were bound to the metal surface, and thus formed inhibition adsorption layer against corrosion.

Recently, Parr et al. [149], have introduced an electrophilicity index (ω) defined as:

$$\omega = \frac{\chi^2}{2\eta} \quad (11)$$

This was proposed as a measure of the electrophilic power of a molecule. The higher the value of ω , the higher the capacity of the molecule to accept electrons. In Eq. (6), χ is electronegativity and η is global hardness. For χ and η , their operational and approximate definitions are [150]: According to Koopmans's theorem [146], the energies of the HOMO and the LUMO orbital's of the inhibitor molecule are related to the ionization potential, I , and the electron affinity, A , respectively. In order to provide a unified treatment of chemical reactivity and selectivity a new concept of philicity has been introduced recently by Chattaraj et al. [151]. This local philicity index is given as:

$$\omega^\alpha(r) = \omega f^\alpha(r) \quad (12)$$

or its condensed-to-atom variant for the atomic site k in a molecule is defined as:

$$\omega_k^\alpha = \omega f_k^\alpha \quad (13)$$

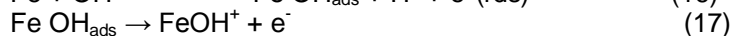
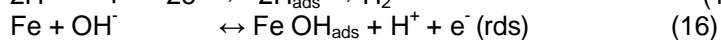
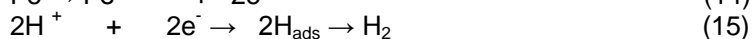
Where $\alpha = +, -, o$ refer to nucleophilic, electrophilic and radical attacks, respectively. The ω_k^α is capable of providing other local and global reactivity descriptors. The electrophilic or nucleophilic power is distributed over all atomic sites in a molecule keeping the overall philicity conserved. The atomic site with the largest ω_k^+ will be the most favorable site for nucleophilic attack, the highest ω_k^- for the electrophilic attack and the highest ω_k^o for the radical attack [151]. It is clear that ω is highest for the protonated form of PSCs inferring that in this form, PSCs has the highest capacity to accept electrons from the vacant d-orbital of iron. According to Wang et al. [150], adsorption of inhibitor onto a metallic surface occurs at the part of the molecule which has the greatest softness and lowest hardness. The results shows that PSCs in the protonated form has the lowest energy gap and lowest hardness; this agrees with the experimental results that PSCs could have better inhibitive performance on iron surface in the protonated form i.e. through electrostatic interaction between the cation form of PSCs and the vacant d-orbital of iron (physisorption). PSCs had the highest inhibition efficiency because it had the highest HOMO energy and ΔN values, and it had the greatest ability of offering electrons. This also agrees well with the value of $\Delta G_{\text{ads}}^\circ$ obtained experimentally [102]. The dipole moment (μ) is another important electronic parameter that results from non-uniform distribution of charges on the various atoms in a molecule. It is mainly used to study the intermolecular interactions involving the Van der Waals type dipole-dipole forces etc., because the larger the dipole moment as shown in Table 1, the stronger will be the intermolecular attraction [145]. The dipole moment of PSCs is highest in the protonated form ($\mu = 8.641$ Debye (28.818×10^{-30} Cm)), which is higher than that of H_2O ($\mu = 6.23 \times 10^{-30}$ Cm). The high value of dipole moment probably increases the adsorption between chemical compound and metal surface [152]. Accordingly, the adsorption of PSC molecules can be regarded as a quasi-substitution process between the PSC compound and water molecules at the electrode surface. Frontier orbital energy level indicates the tendency of bonding to the metal surface. Further study on formation of chelating centers in an inhibitor requires the information of spatial distribution of electronic density of the compound molecules [132]. The

structure of the molecules can affect the adsorption by influencing the electron density at the functional group. Generally, electrophiles attack the molecules at negative charged sites. As seen from Figure 9, the electron density focused on N atoms, O atoms, and C atoms in methyl. The regions of highest electron density are generally the sites to which electrophiles attacked. So, N, O, and C atoms were the active center, which had the strongest ability of bonding to the metal surface. On the other side, HOMO (Figure 7) was mainly distributed on the areas containing aminic nitrogen. Thus, the areas containing N atoms were probably the primary sites of the bonding. As showed in Table 1, the values of HOMO energy increases with increasing length of carbon bone chain containing aminic nitrogen. Similar situation can be also seen in Figures 9 and 10 the configuration changes led to the increase in electron density; and inhibition efficiency was enhanced by increase in HOMO energy and electron density. It is concluded that, the region of active centers transforming electrons from N atoms to iron surface. The electron configuration of iron is [Ar] 4s²3d⁶, the 3d orbitals are not fully filled with electrons. N heteroatom's has lonely electron pairs that is important for bonding unfilled 3d orbitals of iron atom and determining the adsorption of the molecules on the metal surface. PSC_1 had the highest inhibition efficiency among the PSCs, which was resulted from the geometry change that led to HOMO energy increase and electron density distribution in the molecule.

Based on the discussion above, it can be concluded that the PSCs molecules have many active centers of negative charge. In addition, the areas containing N and O atoms are the most possible sites of bonding metal surface by donating electrons to the metal iron.

Chemical and electrochemical measurements

Corrosion inhibition performance of PSCs as corrosion inhibitors was evaluated in details in our previous article [102] using chemical (weight loss and thermometric) and electrochemical techniques. For the chemical methods, a weight measurement is ideally suited for long term immersion test. Corroborative results between weight loss and other techniques have been reported and collected in Tables 2 and 3. The anodic dissolution of iron in acidic and/or alkaline media and the corresponding cathodic reaction has been reported to proceed as follows [153]:



Where 'red' stands for rate-determining step. As a result of these reactions, including the high solubility of the corrosion products, it is evident that [102] the weight loss of iron in the different test solutions increases with time. It may also suggest that the iron corrosion by HNO₃ and NaOH is a heterogeneous process involving several steps. Similar observation has been reported recently [112]. A further inspection of the plots reveal that the weight loss of iron was reduced in the presence of PSCs to the free acid and/or free base solutions at 303 K; an indication of inhibiting effect of acid and alkaline corrosion of iron. The temperature- time curves provide a mean of differentiating between weak and strong adsorption. The thermometric data are depicted in Table 2. It is evident that, the dissolution of iron in 2.0 M HNO₃ starts from the moment of immersion. On increasing the concentration of the inhibitor from (5 x 10⁻⁷ – 1 x 10⁻⁴ M) the value of *T*_{max} decreases, whereas the time (*t*) required reaching *T*_{max} increases, and both factors cause a large decrease in (*RM*) and increasing of (% red *RM*) of the system [117], as shown in Table 2. This indicates that the studied synthesized PSCs retard the dissolution presumably by strongly adsorption onto the metal surface. The extent of inhibition depends on the degree of the surface coverage (*θ*) of the iron surface with the adsorbate. Iron, as an active element, always carries an air formed oxide, which specifically and very strongly adsorbs H⁺ and OH⁻ ions according to the equations (16 - 18), these reactions takes place along the incubation period. The heat evolved from the above reactions accelerates further dissolution of the oxide and activates the dissolution of the iron metal exposed to the aggressive medium.

Kinetics of iron corrosion in HNO₃ with and without PSCs

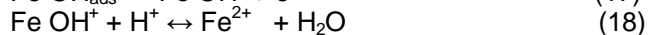
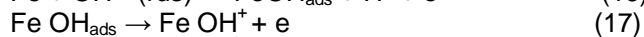
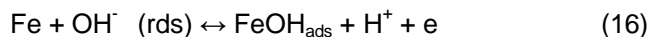
The kinetics of the iron corrosion in the absence and presence of different concentrations of PSCs in 2.0 M HNO₃ was studied at 30 °C by fitting the corrosion data into different rate laws. Correlation coefficients R² were used to determine the best rate law for the corrosion process. The rate laws considered were [154]:

$$\text{Zero-order: } W_t = kt \quad (19)$$

$$\text{First-order: } \ln W_t = -kt + \ln W_0 \quad (20)$$

$$\text{Second-order: } 1/W_t = kt + 1/W_o \quad (21)$$

where W_o is the initial weight of iron, W_t is the weight loss of iron at time t and k is the rate constant. By far best result was obtained for first-order kinetics. The plot of $\ln W_t$ against t which was linear (**Fig. 11**) with good correlation coefficients ($R^2 > 0.9$) confirms first-order kinetics for the corrosion of iron in 2.0 M HNO_3 in the absence and presence of PSC_1. The corrosion rate of iron in nitric acid medium is under anodic control [153] which is:



Where 'rds' stands for rate-determining step

Figure 11 reflects the reaction order with respect to iron. This result suggests that the presence of PSC does not influence the anodic reaction order. The linearity of the curves in the absence and presence of PSC implies that its presence does not change the kinetics of the corrosion reaction though the rate might be considerably reduced. Similar report has been documented elsewhere [155]. The half-life ($t_{1/2}$) value was calculated [156] using the following relationship:

$$t_{1/2} = 0.693/k \quad (22)$$

The values of rate constant and half-life periods obtained are calculated and summarized. The value of the rate constant (k) was found to be higher in the case of inhibited iron samples (0.087) than uninhibited samples (0.049) whereas half-life ($t_{1/2}$) was found to be lower in the presence of inhibitor (8.0 min.) than in its absence (14.0 min.). This implies that the corrosion rate is higher in the absence of inhibitor than with inhibited mild iron samples. Similar results were reported on the kinetics of some organic compounds [30,157]. Another indication of the rate of a first-order reaction is the time constant, τ , [157]. The time required for the concentration of the reactant to fall to $1/e$ of its initial value. The calculated values of the time constants are also presented and correlated. The results show that the time constants were lower (11.58 min.) in the presence of PSC_1 than in its absence (20.26 min.). This confirms that the presence of the PSC inhibitor decreases the dissolution of iron.

Adsorption isotherm and thermodynamic consideration

The adsorption isotherm can be determined if the inhibitor effect is due mainly to the adsorption on the metal surface (i.e. to its blocking). The type of the adsorption isotherm can provide additional information about the properties of the tested PSC compounds. Several adsorption isotherms were assessed, and the Temkin adsorption isotherm was found to provide the best description of the adsorption behavior of the investigated inhibitors. The Temkin isotherm is given by the equation [158]:

$$\exp(f \cdot \theta) = k_{\text{ads}} \cdot C \quad (23)$$

The plots of logarithmic concentration of PSC inhibitors ($\log C$) vs. the surface coverage (Θ) of inhibitors gave straight lines. Consequently, the adsorption of Schiff bases and Schiff base-metal complexes on the surface of iron was found to be governed by the Temkin adsorption isotherm [159] namely:

$$\Theta = a + \ln b C \quad (24)$$

Where C is the concentration of the additive in the bulk of the solution, (Θ) is the degree of coverage of the iron surface by the adsorbed molecules, and a and b are constants. K_{ads} are the equilibrium constant for the adsorption-desorption process and it derivate and tabulated in Table 4. The value of K_{ads} was calculated as 36307 M^{-1} for PSC_1 in HNO_3 acid at 303 K. The relatively high value of adsorption equilibrium constant reflects the high adsorption ability of PSCs on iron surface [160]. The standard free energy of adsorption ($\Delta G_{\text{ads}}^{\circ}$) is related to adsorption constant (K_{ads}) with the following equation [161]:

$$\Delta G_{\text{ads}}^{\circ} = -RT (\ln 55.5 K_{\text{ads}}) \quad (25)$$

Where R is the universal gas constant ($\text{kJ mol}^{-1} \text{K}^{-1}$) and T is the absolute temperature (K). The value of 55.5 is the molar concentration of water in solution expressed in mol L^{-1} . Using the Eq. (25), the calculated values of $\Delta G_{\text{ads}}^{\circ}$ and K_{ads} of

the synthesized PSC inhibitors were listed in Table 4. The negative values of ΔG_{ads}° indicating the spontaneously adsorption of these molecules on the metal surface [162] and strong interactions between inhibitor molecules and the metal surface [163]. The ΔG_{ads}° was calculated as $-16.33 \text{ kJ mol}^{-1}$ for the same compound PSC_1 in HNO_3 acid. The value of ΔG_{ads}° indicates the strong interaction between inhibitor molecules and the Fe surface. Its well known that values of ΔG_{ads}° of the order of $12 - 16 \text{ kJ mol}^{-1}$ or lower in acidic and alkaline solutions (Table 4), indicate a physisorption mechanism. In addition to electrostatic interaction, there may be some other interactions [53,164]. The high K_{ads} and ΔG_{ads}° values may be attributed to higher adsorption of the inhibitor molecules at the metal-solution interface [165]. In physisorption process, it is assumed that acid anions such as NO_3^- ions are specifically adsorbed on the metal surface, donating an excess negative charge to the metal surface. In this way, potential of zero charge becomes less negative which promotes the adsorption of inhibitors in cationic form [166]; those of order of 40 kJ mol^{-1} or higher involve charge sharing or transfer from the inhibitor molecules to the metal surface to form a coordinate type of bond (chemisorptions) [167-169]. Straight lines of C_{inh}/θ versus C_{inh} plots indicate that the adsorption of the inhibitor molecules on the metal surface obeyed Temkin adsorption model (Figure 12). This isotherm can be represented as:

$$C_{inh}/\theta = 1/K_{ads} + C_{inh} \quad (26)$$

The strong correlation coefficients of the fitted curves are around unity ($r = 0.94$). This reveals that the inhibition tendency of the inhibitors is due to the adsorption of these synthesized molecules on the metal surface [170] (Table 4). The slopes of the C_{inh}/θ versus C_{inh} plots are close to $\cong 1.38$ in case of nitric acid; whereas $\cong 2.53$ in the case of NaOH solution which indicates the ideal simulating and expected from Temkin adsorption isotherm [170]. K_{ads} values were calculated from the intercepts of the straight lines on the C_{inh}/θ axis [171]. Generally the relatively high values of the adsorption equilibrium constant (K_{ads}) as given in Table 4 reflect the high adsorption ability [162,163] of the PSC molecules on the iron surface.

To evaluate the kinetic parameters and correlate them to their corrosion inhibition mechanism, it is now of value to analyze the kinetic data obtained in the presence of the studied PSC inhibitors from the stand point of the generalized mechanistic scheme proposed by El-Awady *et al.* [172,173]. The curve fitting of the data for the PSCs on iron in 2.0 M HNO_3 and 2.0 M NaOH solutions to the kinetic-thermodynamic model (equation 28) at 303 K.

$$\theta / (1 - \theta) = K' [I]^y \quad (27)$$

$$\text{or } \log (\theta/1 - \theta) = \log K' + y \log [I] \quad (28)$$

where y is the number of inhibitors molecules [I] occupying one active site, and K' is a constant, if relationship (28) is plotted and applicable [102]. As seen, satisfactory linear relation is observed for the studied synthesized PSC compounds. Hence, the suggested model fits the obtained experimental data. The slope of such lines is the number of inhibitor molecules occupying a single active site, (y) and the intercept is the binding constant ($\log K'$). As mentioned, $1/y$ gives the number of active sites occupied by a single organic molecule and K'^y is the equilibrium constant for the adsorption process. The binding constant (K_b) corresponding to that obtained from the known adsorption isotherms curve fitting is given by the following equation:

$$K_b = K'^{(1/y)} \quad (29)$$

Table 4 comprises the values of $1/y$ and K_b for the studied PSCs. This Table show that the number of active sites occupied by one molecule in the case of PSCs ($1/y \cong 4 - 11$). Values of $1/y$ greater than unity implies the formation of multilayer of the inhibitor molecules on the metal surface, whereas, values of $1/y$ less than unity indicates that a given inhibitor molecule will occupy more than one active site [174]. According to the proposed kinetic-thermodynamic model, the adsorption takes place via formation of multilayer of the inhibitor molecules on the iron electrode surface. The slope values do not equal unity (gradient slopes < 1); hence the adsorption of these synthesized PSCs on iron surface does not obey a Langmuir adsorption isotherm [175,176]. Temkin adsorption isotherm (equation 24) represents best fit for experimental data obtained from applying PSCs as chemical inhibitors on iron in 2.0 M HNO_3 and 2.0 M NaOH solutions. The values of K_{ads} (equilibrium constant of the inhibitor adsorption process) and (f) are tabulated in Table 4. The lateral interaction parameter (f) has negative values; this parameter is a measure of the degree of steepness of the adsorption isotherm. The adsorption equilibrium constant (K_{ads}) calculated from Temkin equation acquires lower values than those binding constant (K_b) obtained and calculated from the kinetic-thermodynamic model. The lack of compatibility of the calculated (K_b) and experimental (K_{ads})

values may be attributed to the fact that Temkin adsorption isotherm is only applicable to cases where one active site per inhibitor molecule is occupied. The lateral interaction model uses the size parameter.

The values of the lateral interaction parameter ($-f$) were found to be negative and increase from ≈ 23 to 38. This denotes that, an increase in the adsorption energy takes place with the increase in the surface coverage (θ). Adsorption process is a displacement reaction involving removal of adsorbed water molecules from the electrode metal surface and their substitution by inhibitor molecules. Thus, during adsorption, the adsorption equilibrium forms an important part in the overall free energy changes in the process of adsorption. It has been shown [177] that, the free energy change (ΔG_{ads}) increases with increase of the solvating energy of adsorbing species, which in turn increases with the size of hydrocarbon portion in the organic molecule and the number of active sites. Hence, the increase of the molecular size leads to decreased solubility, and increased adsorbability. The large negative values of the standard free energy changes of adsorption (ΔG_{ads}), obtained for PSCs, indicate that the reaction is proceeding spontaneously and accompanied with a high efficient adsorption. Although, the obtained values of the binding constant (K_b) from the kinetic model and the modified equilibrium constant (K_{ads}) from Temkin equation are incompatible, generally have large values (Table 4), mean better inhibition efficiency of the investigated synthesized PSCs i.e., stronger electrical interaction between the double layer existing at the phase boundary and the adsorbing molecules. In general, the equilibrium constant of adsorption (K_{ads}) was found to become higher with increasing the inhibition efficiency of the inhibitor studied as shown in Table 4.

Mechanism of corrosion inhibition

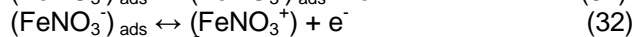
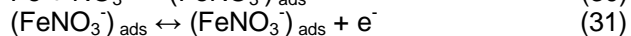
From the experimental and theoretical results obtained, we note that a plausible mechanism of corrosion inhibition of iron in aerated 2.0 M HNO_3 and 2.0 M NaOH by PSCs may be deduced on the basis of adsorption. The transition of metal/solution interface from a state of active dissolution to the passive state is attributed to the adsorption of the inhibitor molecules and the metal surface, forming a protective film [178]. Thermodynamic parameters showed that the adsorption of PSCs on the iron surface either in acidic and/or alkaline solutions is physical than chemical one. The adsorption of PSC arises from the donor

acceptor interactions between free electron pairs of hetero atoms and π electrons of multiple bonds as well as phenyl group and vacant d orbitals of iron [72,179]. It has been reported that the adsorption of heterocyclic compounds occurs with the aromatic rings sometimes parallel but mostly normal to the metal surface. The orientation of molecules could be dependent on the pH and/or electrode potential. However, more work should be completed to confirm the above arguments [180]. In the case of parallel adsorption of inhibitor molecules, the steric factors also must be taken into consideration. The adsorption of organic molecules on the solid surfaces cannot be considered only as purely physical or as purely chemical adsorption phenomenon. In addition to the physical adsorption, inhibitor molecules can also be adsorbed on the iron surface via

electrostatic interaction between the charged metal surface and charged inhibitor molecule if it is possible. The calculated standard free energy of adsorption has been found close to -17 kJ mol^{-1} (Table 4) which can be explained as physical rather than chemical adsorption. If the contribution of electrostatic interactions takes place, the following adsorption process can additionally be discussed. The essential effect of Schiff bases as corrosion inhibitors is due to the $\text{C}=\text{N}$ group in the molecules Schiff bases, π electrons on the aromatic rings, mode of interaction with the metal surface and the formation of metallic complexes [64,181–182]. The unshared and π electrons interact with d orbital of Fe to provide a protective film. Five Schiff bases investigated in the present study have one, two, and/or three benzene rings; one hetero nitrogen-five member ring and $\text{C}=\text{N}$ group. The optimized geometry of Schiff bases (PSC_1–5) is presented in Fig. 10. According to Fig. 10 each molecule of Schiff bases has an OH group in the ortho position for PSC_1–4, and in para position for PSC_5, one group $\text{C}=\text{N}$ presence between benzene rings and the hetero nitrogen-five member ring. In addition, PSCs_1 and PSCs_2 has an excess O atom in the ortho position and two CH_3 groups in o- and m-positions at the hetero nitrogen-five member ring linked to carbon of $\text{C}=\text{N}$ group. The inhibition efficiency values of five Schiff bases (PSC_1–5) at a common concentration of 0.1 mM (Table 3) follow the order: Schiff base_1 > Schiff base_2 > Schiff base_3 > Schiff base_4 > Schiff base_5. The quantum results were used to explain different inhibition effectiveness of the five molecules. From optimized geometry of Schiff bases (PSC_1–5) (Fig. 10), it can be observed that all these five molecules have approximate planar structure. Thus, the adsorption of studied Schiff bases on iron surface would take place through $\text{C}=\text{N}$ groups, benzene rings, methyl and hydroxyl functional groups. PSC_1 and 2 have the highest percentage inhibition efficiency. This is due to the large size of antipyrine category which makes better surface coverage and hence the highest inhibition efficiency is obtained. PSC_1 displays the highest inhibition efficiency; this is due to the presence of additional benzene ring in its structure which enhances the electron density on the inhibitor in addition to its higher molecular area. The inhibition efficiency of PSC_3 is higher than that of PSC_4, due to the presence of an additional benzene ring in the arylidene part of the additive, which increases the area of the adsorbed molecule and consequently makes better surface coverage on the metal surface than in the case of the other additives PSC_4 and PSC_5. The inhibition efficiency of PSC_4 is higher than that of compound PSC_5, which can

be explained on the basis that, the basic strength of the C = N group is insufficient to permit the formation of stable complex through a simple coordination bond with the metal ion through the lone pair of the nitrogen atom. Therefore, a functional group with a replaceable hydrogen ion (OH group) in the ortho position of PSC_4 enhances the formation of a stable chelate complex with the corroding metal ions. Consequently, both the Schiff base inhibitor and Schiff base-metallocomplexes can be adsorbed or deposited on the metal surface, hence causing an additional inhibition of iron corrosion [62,183]. Finally, PSC_5 comes at the end of all the investigated PSC compounds in its percentage inhibition efficiency value, owing to the presence of OH group in the para position. The adsorption process of PSC molecules on the metal surface interfere with the adsorption of the anions [173] present in the corrosive media.

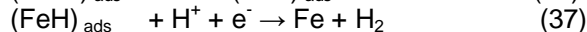
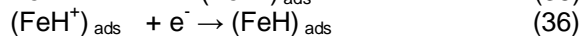
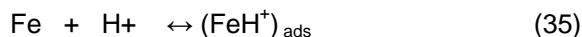
The anodic dissolution of iron follows the steps [184]:



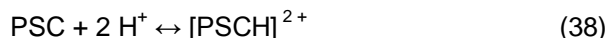
Schiff bases have basic character and expected to be protonated in equilibrium with the corresponding neutral form in strong acid solutions.



Because iron surface carried positive charge, NO_3^- ions should be first adsorbed onto the positively charged metal surface according to reaction (30). Then the inhibitor molecules adsorb through electrostatic interactions between the negatively charged metal surface and positively charged Schiff base molecule (PSCH^+) and form a protective $(\text{FeNO}_3^- \text{PSCH}^+)_{\text{ads}}$ layer. In this way, the oxidation reaction of $(\text{FeNO}_3^-)_{\text{ads}}$ as shown by reaction steps from (31) to (33) can be prevented [3,185]. During the corrosion of iron in strong acid solution, the cathodic reaction is reduction of H^+ ions to molecular hydrogen according to reaction mechanism given below [3,184]:



Because the rate of hydrogen gas evolution is directly proportional to the rate of corrosion, the measuring of hydrogen gas evolved at cathodic sites as a function of reaction time can give valuable information about starting and continuity of the corrosion. The relative speed and effectiveness of the gasometric techniques as well as their suitability for in situ monitoring, any perturbation by an inhibitor with respect to gas evolution in metal/solution system has been established in the literature [4,186-189]. The protonated Schiff base molecules are also adsorbed at cathodic sites of metal in competition with hydrogen ions according to Eq. (35). The adsorption of protonated Schiff base molecules reduces the rate of hydrogen evolution reaction [179,184,190]. In acidic solutions the inhibitor can exist as cationic species (Eq. (38)) which may be adsorbed on the cathodic sites of the iron and reduce the evolution of hydrogen:



The protonated PSC, however, could be attached to the iron surface by means of electrostatic interaction between NO_3^- and protonated PSC since the iron surface has positive charges in the acid medium [191]. This could further be explained based on the assumption that in the presence of NO_3^- , the negatively charged

NO_3^- would attach to positively charged surface. When PSC adsorbs on the iron surface, electrostatic interaction takes place by partial transference of electrons from the polar atoms (N and O atoms and the delocalized π -electrons around the heterocyclic rings) of PSC to the metal surface. In addition to electrostatic interaction (physisorption) of PSC molecules on the iron surface, molecular adsorption may also play a role in the adsorption process. A close examination of the chemical structure of PSCs, reveals that PSC molecules have structure characterized by the presence of chelation centers mainly located on nitrogen's and oxygen. From theoretical and experimental results obtained, N and O atoms are the likely sites of complexation of PSC with the Fe^{2+} (**Fig.13**) which will result in the formation of a five-membered, redox active α -iminoketo chelate ring [192]. The UV-Visible absorption spectra of the solution containing the inhibitor after the immersion of the iron specimen indicated the formation of a complex with the iron surface allowing the formation of adhesive film. Such an adhesive film covered the metal surface isolating the metal surface from the corrosive media. Finally, it should also be emphasized that, the large size and high molecular weight of Schiff base

molecule can also contribute the greater inhibition efficiency of PSCs [72]. In order to present more details, the molecular orbital density distributions for five Schiff bases are shown. **Figures 7, 8** shows that all of investigated Schiff bases (PSC_1-5) have very similar electronic density on their HOMO, so different inhibition effectiveness observed in five molecules cannot be explained in terms of E_{HOMO} . However, it can be found in **Figures 7, 8** that the orbital density distributions on LUMO of these five Schiff bases are similar to each other and their only difference is related to orbital density distributions of LUMO that is localized over the atoms N and O and follows the following order: Schiff base_1 > Schiff base_2 > Schiff base_3 > Schiff base_4 > Schiff base_5. Finally, we remark that we do not know the real structure of Schiff base films; instead these arguments are used to demonstrate the differences in inhibition efficiency of these molecules.

In general, the adsorption of organic molecules at the metal electrode surface depends on the molecular size, charge distribution and deformability of the active center as well as the charge on the metal surface undergoing corrosion. Thus, the increased formation of Schiff base-metal complexes leads to the formation of an insoluble film of the complex on the metal surface, which furnishes an additional inhibitive property to that of the investigated Schiff base inhibitors (PSCs) as shown in Figure 13.

CONCLUSIONS

Data obtained from quantum chemical calculations using DFT at the B3LYP/6-311++G** level of theory were correlated to the inhibitive effect of Schiff bases (PSCs). The relationships between inhibition efficiency of iron in aerated 2.0 M HNO_3 and/or 2.0 M NaOH and the E_{HOMO} , $E_{\text{LUMO}} - E_{\text{HOMO}}$, and ΔN of PSCs were calculated by DFT method. The inhibition efficiency increased with the increase in E_{HOMO} and decrease in $E_{\text{LUMO}} - E_{\text{HOMO}}$. PSC_1 had the highest inhibition efficiency because it had the highest HOMO energy and ΔN values, and it was most capable of offering electrons. The distribution of electronic density shows that the molecules of PSCs had many negatively-charged active centers. The electron density was found to be positively correlated with length of aminic nitrogen containing carbon bone chain, which was resulted in increasing in inhibition efficiency. The areas containing N and O atoms are most possible sites for bonding the metal iron surface by donating electrons to the metal. The inhibition efficiencies obtained from chemical and electrochemical methods are in good agreement with each other. Its inhibition efficiency is both concentration and immersion time dependent. The high inhibition efficiency of PSCs was attributed to the adherent adsorption of the inhibitor molecules on the metal surface, and the adsorption is spontaneous, exothermic; accompanied with a decrease in entropy of the system from thermodynamic point of view and obeys the Temkin isotherm. Polarization curves demonstrate that the examined Schiff bases behave as mixed type corrosion inhibitor in HNO_3 by inhibiting both anodic metal dissolution and cathodic hydrogen evolution reactions. A first-order kinetics relationship with respect to the iron was obtained with and without PSC from the kinetic treatment of the data. UV-Visible spectrophotometric studies clearly reveal the formation of Fe-PSC complex which may be enhanced for the observed inhibition process. Both experimental and quantum theoretical calculations are in excellent agreement.

ACKNOWLEDGEMENTS

I gratefully acknowledge Tanta University, Chemistry Department, Tanta, Egypt for the financial assistance and Department of Chemistry, King Abdul-Aziz University, Jeddah, Saudi Arabia for facilitation of our study.

References

- [1] Doner A, Sahin EA, Kardas G, Serindag O (2013). "Investigation of corrosion inhibition effect of 3-[(2-hydroxy-benzylidene)-amino]-2thioxo-thiazolidin-4-one on corrosion of mild steel in the acidic Medium". *Corros. Sci.* 66: 278-284.
- [2] Doner A, Solmaz R, Ozcan M, Kardas G (2011). "Experimental and theoretical studies of thiazoles as corrosion inhibitors for mild steel in sulphuric acid solution". *Corros. Sci.* 53:2902-2913.
- [3] Solmaz R, Kardas G, Culha M, Yazıcı B, Erbil M (2008). "Investigation of adsorption and inhibitive effect of 2-mercaptothiazoline on corrosion of mild steel in hydrochloric acid media". *Electrochim. Acta* 53: 5941-5952.
- [4] Solmaz R, Mert ME, Kardas G, Yazıcı B, Erbil M (2008). "Adsorption and Corrosion Inhibition Effect of 1,1'-Thiocarbonyldiimidazole on Mild Steel in H_2SO_4 Solution and Synergistic Effect of Iodide Ion". *Acta Chim. Sinica* 24: 1185-1191.
- [5] Altunbas E, Solmaz R, Kardas G (2010). "Corrosion behaviour of polyrhodanine coated copper electrode in 0.1 M H_2SO_4 solution". *Mater. Chem. Phys.* 121: 354-358.
- [6] Elachouri M, Kertit S, Gouttaya HM, Nciri B, Bensouda Y, Perez L, Infante MR, Elkacemi K (2001). "Corrosion inhibition of iron in 1 M HCl by some gemini surfactants in the series of alkanediyl- α , ω -bis(dimethyltetradecyl ammonium bromide)". *Prog. Org. Coat.* 43: 267-273.
- [7] Mernari B, El Attari H, Traisnel M, Bentiss F, Lagrenee M (1998). "Inhibiting effects of 3,5-bis(n-pyridyl)-4-amino-1,2,4-triazoles on the corrosion of mild steel in 1 M HCl medium". *Corros. Sci.* 40: 391-399.

- [8] Avcı G (2008). "Corrosion inhibition of indole-3-acetic acid on mild steel in 0.5 M HCl". *Colloids Surf. A* 317: 730–736.
- [9] Solmaz R, Sahin EA, Döner A, Kardas G (2011). —The investigation of synergistic inhibition effect of rhodanine and iodide ion on the corrosion of copper in sulphuric acid solution. *Corros. Sci.* 53:3231–3240.
- [10] Negm NA, Elkholy YM, Zahran MK, Tawfik SM (2010). "Corrosion inhibition efficiency and surface activity of benzothiazol-3-ium cationic Schiff base derivatives in hydrochloric acid". *Corros. Sci.* 52: 3523-3536.
- [11] Ameer MA, Khamis E, Al Senani G (2000). "Adsorption studies of the effect of thiosemicarbazides on the corrosion of steel in phosphoric acid". *Adsorpt. Sci. Technol.* 18: 177–189.
- [12] Kissi M, Bouklah M, Hammouti B, Benkaddour M (2006). "Establishment of equivalent circuits from electrochemical impedance spectroscopy study of corrosion inhibition of steel by pyrazine in sulphuric acidic solution". *Appl. Surf. Sci.* 252: 4190–4198.
- [13] Oguzie EE, Onuoha GN, Onuchukwu AI (2004). "Inhibitory mechanism of mild steel corrosion in 2 M sulphuric acid solution by methylene blue dye". *Mater. Chem. Phys.* 89: 305–311.
- [14] Oguzie EE (2005). "Corrosion inhibition of mild steel in hydrochloric acid solution by methylene blue dye". *Mater. Lett.* 59: 1076–1079.
- [15] Tang L, Li X, Mu G, Liu G, Li L, Liu H, Si Y (2006). "The synergistic inhibition between hexadecyltrimethyl ammonium bromide (HTAB) and NaBr for the corrosion of cold rolled steel in 0.5 M sulfuric acid". *J. Mater. Sci.* 41: 3063–3069.
- [16] Ebenso EE (2003). —Effect of halide ions on the corrosion inhibition of mild steel in H₂SO₄ using methyl red: Part 1 —. *Bull. Electrochem.* 19: 209–216.
- [17] Zhang DQ, Gao LX, Zhou GD (2003). —Synergistic effect of 2-mercapto benzimidazole and KI on copper corrosion inhibition in aerated sulfuric acid solution. *J. Appl. Electrochem.* 33: 361–366.
- [18] Harek Y, Larabi L (2004). —Role of Some Benzohydrazide Derivatives as Corrosion Inhibitors for Carbon Steel in HCl Solution. *Kem. Ind.* 53 (2): 55–63.
- [19] Behpour M, Ghoreis SM, Mohammad N, Soltani N, Salavati-Niasari MM (2010). —Investigation of some Schiff base compounds containing disulfide bond as HCl corrosion inhibitors for mild steel. *Corros. Sci.* 52: 4046-4057.
- [20] Aljourani J, Raeissi K, Golozar MA (2009). —Benzimidazole and its derivatives as corrosion inhibitors for mild steel in 1M HCl solution. *Corros. Sci.* 51: 1836.
- [21] Emregül KC, Atakol O (2003). —Corrosion inhibition of mild steel with Schiff base compounds in 1 M HCl. *Mater. Chem. Phys.* 82: 188.
- [22] Asan A, Kabasakaloglu M, Iskanal M, Kılıç Z (2005). —Corrosion inhibition of brass in presence of terdentate ligands in chloride solution. *Corros. Sci.* 47 (6): 1534.
- [23] Stanly JK, Parameswaran G (2010). —Corrosion inhibition of mild steel in hydrochloric acid solution by Schiff base furointhiosemicarbazone. *Corros. Sci.* 224.
- [24] Tang Y, Yang X, Yang W, Chen Y, Wana R (2010). —Experimental and molecular dynamics studies on corrosion inhibition of mild steel by 2-amino-5 phenyl-1, 3, 4-thiadiazole. *Corros. Sci.* 52: 242.
- [25] Lowmunkhong P, Ungthararak D, Sutthivaiyakit P (2010). "Tryptamine as a corrosion inhibitor of mild steel in hydrochloric acid solution". *Corros. Sci.* 52: 30.
- [26] Abdallah M (2002). —Rhodanine azosulpha drugs as corrosion inhibitors for corrosion of 304 stainless steel in hydrochloric acid solution. *Corros. Sci.* 44: 717.
- [27] Hegazy MA (2009). —A novel Schiff base-based cationic Gemini surfactants: Synthesis and effect on corrosion inhibition of carbon steel in hydrochloric acid solution. *Corros. Sci.* 51: 2610.
- [28] Hasanov R, Bilge S, Bilgiç S, Gece G, Kılıç Z (2010). —Experimental and theoretical calculations on corrosion inhibition of steel in 1M H₂SO₄ by crown type polyethers. *Corros. Sci.* 52: 984.
- [29] Chetouani A, Aouniti A, Hammouti B, Benchat N, Benhadda T, Kertit S (2003). —Corrosion inhibitors for iron in hydrochloric acid solution by newly synthesized pyridazine derivatives. *Corros. Sci.* 45: 1675.
- [30] Obi-Egbedi NO, Obot IB (2011). —Inhibitive properties, thermodynamic and quantum chemical studies of alloxazine on mild steel corrosion in H₂SO₄. *Corros. Sci.* 53: 263-275.
- [31] Obot IB, Obi-Egbedi NO, Odozi NW (2010). —Acenaphtho [1,2-b] quinoxaline as a novel corrosion inhibitor for mild steel in 0.5 M H₂SO₄. *Corros. Sci.* 52: 923.
- [32] Obot IB, Obi-Egbedi NO (2010). —2,3-Diphenylbenzoquinoxaline: A new corrosion inhibitor for mild steel in sulphuric acid. *Corros. Sci.* 52: 282–285.
- [33] Obot IB, Obi-Egbedi NO (2008). —Inhibitory Effect and Adsorption Characteristics of 2,3-Diaminonaphthalene At Aluminum/Hydrochloric Acid Interface: Experimental and Theoretical Study. *Surf. Rev. Lett.* 15 (6): 903–910.
- [34] Quraishi MA, Ansari FA (2006). —Fatty acid oxadiazoles as corrosion inhibitors for mild steel in formic acid. *J. Appl. Electrochem.* 36:309–314.
- [35] Quraishi MA, Rafiquee MZA, Saxena N, Khan S (2006). —Fatty acid oxadiazoles as corrosion inhibitors for mild steel in formic acid —. *J. Corros. Sci. Eng.*: 10–16. doi: 10.1007/s10800-005-9065-z
- [36] Abd El Rehim SS, Hassan HH, Amin MA (2003). —The corrosion inhibition study of sodium dodecyl benzene sulphonate to aluminium and its alloys in 1.0 M HCl solution. *Mater. Chem. Phys.* 78: 337–348.
- [37] Bentiss F, Traisnel M, Chaibi N, Merna B, Vezin H, Lagrenee M (2002). —2,5-Bis(n-methoxyphenyl)-1,3,4-oxadiazoles used as corrosion inhibitors in acidic media: correlation between inhibition efficiency and chemical structure. *Corros. Sci.* 44: 2271–2289.
- [38] Lebrini M, Lagrenee M, Vezin H, Gengembre L, Bentiss F (2005). —Electrochemical and quantum chemical studies of new thiadiazole derivatives adsorption on mild steel in normal hydrochloric acid medium. *Corros. Sci.* 47: 485–505.
- [39] Ahmed AI, El-Askany AH, Fouda AS (1985). —Effect of some hydrazone compounds on the corrosion behaviour of aluminum in HCl and NaOH solutions. *J. Indian Chem. Soc.* 22: 367–374.
- [40] Pei ZT, Guan NM (1999). —The adsorption and corrosion inhibition of anion surfactants on aluminium surface in hydrochloric acid. *Corros. Sci.* 41: 1937–1944.
- [41] Fouda AS, El-Semongy MM (1982). —The effect of some amino acids on the corrosion of aluminum in hydrochloric acid solution. *J. Indian Chem. Soc.* 19: 89–96.
- [42] Garrigues L, Pebere, Dabosi F (1996). —An investigation of the corrosion inhibition of pure aluminum in neutral and acidic chloride Solutions. *Electrochim. Acta* 41: 1209-1215.
- [43] Obot IB, Obi-Egbedi NO (2008). —Fluconazole as an inhibitor for aluminium corrosion in 0.1 M HCl —. *Colloids Surf. A Physicochem. Eng. Aspects* 330: 207–212. doi: 10.1016/j.colsurfa.2008.07.058
- [44] Obot IB, Obi-Egbedi NO, Umoren SA (2009). —The synergistic inhibitive effect and some quantum chemical parameters of Clotrimazole for Aluminium Corrosion in Hydrochloric Acid. *Int. J. Electrochem. Sci.* 4: 863–877.

- [45] Obot IB, Obi-Egbedi NO (2010). Adsorption properties and inhibition of mild steel corrosion in sulphuric acid solution by ketoconazole: Experimental and theoretical investigation. *Corros. Sci.* 52: 198–204.
- [46] Obot IB, Obi-Egbedi NO, Umoren SA (2009). —Antifungal drugs as corrosion inhibitors for aluminium in 0.1 M HCl. *Corros. Sci.* 51:1868–1875.
- [47] Obot IB, Port (2009). Synergistic effect of nizarol and iodide ions on the corrosion inhibition of mild steel in sulphuric acid solution — *Electrochim. Acta* 27(5): 539–553. http://www.peacta.org/articles_upload/PEA_27_5_2009_539_553.pdf doi: 10.4152/pea.200905539
- [48] Obot IB, Obi-Egbedi NO, Umoren SA (2009). —The synergistic inhibitive effect and some quantum chemical parameters of 2,3-diaminonaphthalene and iodide ions on the hydrochloric acid corrosion of aluminium. *Corros. Sci.* 51: 276–282.
- [49] Obot IB, Obi-Egbedi NO (2010). —Theoretical study of benzimidazole and its derivatives and their potential activity as corrosion inhibitors. *Corros. Sci.* 52: 657–660.
- [50] Ebenso EE, Alemu H, Umoren SA, Obot IB (2008). “Inhibition of Mild Steel Corrosion in Sulphuric Acid Using Alizarin Yellow GG Dye and Synergistic Iodide Additive”. *Int. J. Electrochem. Sci.* 4: 1325–1339.
- [51] Behpour M, Ghoreishi SM, Gandomi-Niasari A, Soltani N, Salavati-Niasari M (2009). — The inhibition of mild steel corrosion in hydrochloric acid media by two Schiff base compounds. *J. Mater. Sci.* 44: 2444–2453.
- [52] Asan A, Soylu S, Kiyak T, Yıldırım F (2006). —Investigation on some Schiff bases as corrosion inhibitors for mild steel. *Corros. Sci.* 48:3933.
- [53] Behpour M, Ghoreishi SM, Soltani N, Salavati-Niasari M, Hamadanian M, Gandomi A (2008). Electrochemical and theoretical investigation on the corrosion inhibition of mild steel by thiosalicylaldehyde derivatives in hydrochloric acid solution. *Corros. Sci.* 50(8): 2172–2181.
- [54] Abdel-Gaber AM, Masoud MS, Khalil EA, Shehata EE (2009).—Electrochemical study on the effect of Schiff base and its cobalt complex on the acid corrosion of steel. *Corros. Sci.* 51: 3021.
- [55] Chitra S, Parameswari K, Selvaraj A (2010). —Dianiline Schiff Bases as Inhibitors of Mild Steel Corrosion in Acid Media. *Int. J. Electrochem. Sci.* 5: 1675–1697.
- [56] Solmaz R (2010). —Investigation of the inhibition effect of 5-((E)-4-phenylbuta-1,3-dienylideneamino)-1,3,4-thiadiazole-2-thiol Schiff base on mild steel corrosion in hydrochloric acid. *Corros. Sci.* 52: 3321–3330.
- [57] Solmaz R, EceAltunbaş, Kardas G (2011). RamazanSolmaza, Corresponding author contact information, E-mail the corresponding author, Adsorption and corrosion inhibition effect of 2-((5-mercapto-1,3,4-thiadiazol-2-ylimino)methyl)phenol Schiff base on mild steel, GülfezaKardaş. *Mater. Chem. Phys.* 125: 796–801.
- [58] Hosseini MG, Ehteshamzadeh M, Shahrabi T (2007). Protection of mild steel corrosion with Schiff bases in 0.5 M H₂SO₄ solution. *Electrochim. Acta* 52: 3680–3685.
- [59] Álvarez-Bustamante R, Negrón-Silva G, Abreu-Quijano M, Herrera-Hernández H, Romero-Romo M, Cuán A, Palomar-Pardavé M (2009). Electrochemical study of 2-mercaptoimidazole as a novel corrosion inhibitor for steels. *Electrochim. Acta* 54: 5393–5399.
- [60] Negm NA, Zaki MF (2008).—Corrosion inhibition efficiency of nonionic Schiff base amphiphiles of p-aminobenzoic acid for aluminum in 4N HCl. *Colloid Surf. A* 322: 97–102.
- [61] Ehteshamzadeh M, Jafari AH, Esmaeel N, Hosseini MG (2009).—Effect of carbon steel microstructures and molecular structure of two new Schiff base compounds on inhibition performance in 1 M HCl solution by EIS. *Mater. Chem. Phys.* 113: 986–993.
- [62] Shokry H, Yuasa M, Sekine I, Issa RM, El-Baradie HY, Gomma GK (1998). —Corrosion inhibition of mild steel by schiff base compounds in various aqueous solutions: part 1. *Corros. Sci.* 40: 2173–2186.
- [63] Emregül KC, Hayvali M (2006). —Studies on the effect of a newly synthesized Schiff base compound from phenazone and vanillin on the corrosion of steel in 2 M HCl. *Corros. Sci.* 48: 797–812.
- [64] Behpour M, Ghoreishi SM, Soltani N, Salavati-Niasari M (2009). The inhibitive effect of some bis-N,S-bidentate Schiff bases on corrosion behaviour of 304 stainless steel in hydrochloric acid solution. *Corros. Sci.* 51: 1073–1082.
- [65] Hong Ju, Zhen-Peng K, Yan Li (2008). —Aminic nitrogen-bearing polydentate Schiff base compounds as corrosion inhibitors for iron in acidic media: A quantum chemical calculation. *Corros. Sci.* 50: 865–871.
- [66] Li S, Chen S, Lei S, Ma H, Yu R, Liu D (1999). —Investigation on some Schiff bases as HCl corrosion inhibitors for copper. *Corros. Sci.* 41: 1273–1287.
- [67] Emregül KC, Atakol O (2004). —Corrosion inhibition of iron in 1 M HCl solution with Schiff base compounds and derivatives. *Mater. Chem. Phys.* 83: 373–379.
- [68] Emregül KC, Kurtaran R, Atakol O (2003). —An investigation of chloride-substituted Schiff bases as corrosion inhibitors for steel. *Corros. Sci.* 45: 2803–2817.
- [69] Asan A, Soylu S, Kiyak T, Yıldırım F (2006). Investigation on some Schiff bases as corrosion inhibitors for mild steel. *Corros. Sci.* 48: 3933–3944.
- [70] Yurt A, Ulutas S, Dal H (2006). —Electrochemical and theoretical investigation on the corrosion of aluminium in acidic solution containing some Schiff bases. *Appl. Surf. Sci.* 253: 919–925.
- [71] Emregül KC, Düzgün E, Atakol O (2006). —The application of some polydentate Schiff base compounds containing aminic nitrogens as corrosion inhibitors for mild steel in acidic media. *Corros. Sci.* 48: 3242–3260.
- [72] Behpour M, Ghoreishi SM, Salavati-Niasari M, Ebrahimi B (2008).—Evaluating two new synthesized S–N Schiff bases on the corrosion of copper in 15% hydrochloric acid. *Mater. Chem. Phys.* 107: 153–157.
- [73] Prabhu RA, Venkatesha TV, Shanbhag AV, Praveen BM, Kulkarni GM, Kalkhambkar RG (2008). —Quinol-2-thione compounds as corrosion inhibitors for mild steel in acid solution. *Mater. Chem. Phys.* 108:283–289.
- [74] Quartarone G, Bonaldo L, Tortato C (2006). —Inhibitive action of indole-5-carboxylic acid towards corrosion of mild steel in deaerated 0.5 M sulfuric acid solutions. *Appl. Surf. Sci.* 252: 8251–8257.
- [75] Bentiss F, Mernari B, Traisnel M, Vezin H, Lagrenée M (2011). On the relationship between corrosion inhibiting effect and molecular structure of 2,5-bis-(n-pyridyl)-1,3,4-thiadiazole derivatives in acidic media: Ac impedance and DFT studies. *Corros. Sci.* 53: 487–495.
- [76] Bentiss F, Lebrini M, Lagrenée M (2005). —Thermodynamic characterization of metal dissolution and inhibitor adsorption processes in mild steel/2,5-bis-(n-thienyl)-1,3,4-thiadiazoles/hydrochloric acid system. *Corros. Sci.* 47: 2915.
- [77] Bentiss F, Gassama F, Barbry D, Gengembre L, Vezin H, Lagrenée M, Traisnel M (2006). —Enhanced corrosion resistance of mild steel in molar hydrochloric acid solution by 1,4-bis(2-pyridyl)-5Hpyridazino[4,5-b]indole: Electrochemical, theoretical and XPS Studies. *Appl. Surf. Sci.* 252: 2684.
- [78] Khaled KF, Babic-Samradzija K, Hackerman N (2005). —Theoretical study of the structural effects of polymethylene amines on corrosion inhibition of iron in acid solutions. *Electrochim. Acta* 50: 2515.
- [79] Wang H, Liu R, Xin J (2004). —Inhibiting effects of some mercaptotriazole derivatives on the corrosion of mild steel in 1.0 M HCl medium. *Corros. Sci.* 46: 2455.
- [80] Bentiss F, Bouanis M, Mernari B, Traisnel M, Lagrenée M (2002).—Effect of iodide ions on corrosion inhibition of mild steel by 3,5-bis(4-methylthiophenyl)-4H-1,2,4-triazole in sulfuric acid solution. *J. Appl. Electrochem.* 32: 671.

- [81] Chetouani A, Hammouti B, Aouniti A, Benchat N, Benhadda T (2002).—New synthesized pyridazine derivatives as effective inhibitors for the corrosion of pure iron in HCl medium. *Prog. Org. Coat.* 45: 373.
- [82] Quraishi MA, Jamal D (2002). —Inhibition of mild steel corrosion in the presence of fatty acid triazoles. *J. Appl. Electrochem.* 32: 425.
- [83] Bouklah M, Hammouti B, Aouniti A, Benhadda T (2004). "Thiophen derivatives as effective inhibitors for the corrosion of steel in 0.5 M H₂SO₄". *Prog. Org. Coat.* 49: 225.
- [84] Popova A, Christov M, Raicheva S, Sokolova E (2004). —Adsorption and inhibitive properties of benzimidazole derivatives in acid mild steel corrosion. *Corros. Sci.* 46: 1333.
- [85] Lebrini M, Traisnel M, Lagrenée M, Mernari B, Bentiss F (2008). "Inhibitive properties, adsorption and a theoretical study of 3,5-bis(npyridyl)-4-amino-1,2,4-triazoles as corrosion inhibitors for mild steel in perchloric acid". *Corros. Sci.* 50: 473.
- [86] Bereket G, Ögretir C, Yurt A (2001). —Quantum mechanical calculations on some 4-methyl-5-substituted imidazole derivatives as acidic corrosion inhibitor for zinc. *J. Mol. Struct. (THEOCHEM)* 571: 139.
- [87] Khalil N (2003). "Quantum chemical approach of corrosion inhibition". *Electrochim. Acta* 48: 2635.
- [88] Costa JM, Lluch JM (1984). —The use of quantum mechanics calculations for the study of corrosion inhibitors. *Corros. Sci.* 24: 929.
- [89] Vasseghi S, Nobe K (1979). "EFFECT OF SUBSTITUTED PURINES ON THE CORROSION BEHAVIOR OF IRON". *Corrosion* 35 (7): 300-303.
- [90] Vosta J, Eliasek J (1971). —STUDY ON CORROSION INHIBITION FROM ASPECT OF QUANTUM CHEMISTRY". *Corrosion* 11: 223.
- [91] El Sayed H, El Ashry, Ahmed El Nemr, Sami A. Esawy, Safaa Ragab (2006). "Corrosion inhibitors". *Electrochim. Acta* 51: 3957–3968.
- [92] Zhao P, Liang Q, Li Y (2005). —Electrochemical, SEM/EDS and quantum chemical study of phthalocyanines as corrosion inhibitors for mild steel in 1 mol/l HCl. *Appl. Surf. Sci.* 252: 1596–1607.
- [93] Xiao-Ci Y, Hong Z, Ming-Dao L, Hong-Xuang R, Lu-An (2000).—Quantum chemical study of the inhibition properties of pyridine and its derivatives at an aluminum surface. *Corros. Sci.* 42: 645–653.
- [94] Daxi W, Shuyuan Li, Yu Y, Mingjun W, Heming X, Zhaoxu C (1999).—Theoretical and experimental studies of structure and inhibition efficiency of imidazoline derivatives. *Corros. Sci.* 41: 1911–1919. doi:10.1016/j.matchemphys.2009.05.043.
- [95] Bereket G, Hür E, Ögretir C (2002). —Quantum chemical studies on some imidazole derivatives as corrosion inhibitors for iron in acidic medium. *J. Mol. Struct. (THEOCHEM)* 578: 79–88.
- [96] Ögretir C, Mihçi B, Bereket G (1999). —Quantum chemical studies of some pyridine derivatives as corrosion inhibitors. *J. Mol. Struct. (THEOCHEM)* 488 : 223–231.
- [97] Chakrabarti A (1984). —Quantum-Chemical Study of the Corrosion Inhibition of Mild Steel in 6% (wt/wt) HCl by means of Cyanoguanidine Derivatives. *Br. Corros. J.* 19: 124.
- [98] Abdul-Ahad PG, Al-Madfaï SHF (1989). —Elucidation of Corrosion Inhibition Mechanism by Means of Calculated Electronic Indexes. *Corrosion* 45 (12): 978.
- [99] Growcock FB (1989). —Inhibition of Steel Corrosion in HCl by Derivatives of Cinnamaldehyde: Part I. Corrosion Inhibition Model. *Corrosion* 45 (12): 1003.
- [100] Sayos R, Gonzalez M, Costa JM (1986). —On the use of quantum chemical methods as an additional tool in studying corrosion inhibitor substances. *Corros. Sci.* 26: 927.
- [101] El Ashry EH, El Nemr A, Esawy SA, S. Ragab S (2006). —Corrosion Inhibitors. *Electrochim. Acta* 51: 957.
- [102] Madkour LH, Zinhome UA (2010). "Inhibition effect of Schiff base compounds on the corrosion of iron in nitric acid and sodium hydroxide solutions". *J. Corr. Sci. Eng. (JCSE)* 13.
- [103] Çukurovalı A, Yılmaz I, Gur S, Kazaz C (2006). —Synthesis, antimicrobial and antifungal activity of some new thiazoly lhydrazone derivatives containing 3-substituted cyclobutane ring. *European Journal of Medicinal Chemistry*, 41(2): 201-207.
- [104] Ozbey S, Temel A, Ancin N, Oztas SG, Tuzun M, Z. Kristallogr Z (1998) " Investigation of some Schiff base compounds containing disulfide bond as HCl corrosion inhibitors for mild steel". *New Cryst. Struct.* 213207.
- [105] Oztas S, Ancin G, Tuzun NM (1997). " Acta Crystallographica Section E: 1,2-Bis[2-[(4-methoxybenzylidene)amino]phenyl]disulfane". *Acta Crystallogr. C* 53: 376.
- [106] Musa AY, Khadom AA, Kadhum AH, Mohamad AB, Takriff MS (2010). —Kinetic behavior of mild steel corrosion inhibition by 4-amino-5-phenyl-4H-1,2,4-triazole-3-thiol. *J. Taiwan, Ins. Chem. Eng.* 41: 126–128.
- [107] Khadom AA, Yaro AS, Kadum AH, Taiwan J (2010). —Corrosion inhibition by naphthylamine and phenylenediamine for the corrosion of copper-nickel alloy in hydrochloric acid. *Ins. Chem. Eng.* 41: 122–125.
- [108] Bouklah M, Hammouti B, Lagrenée M, Bentiss F (2006). "Thermodynamic properties of 2,5-bis(4-methoxyphenyl)-1,3,4-oxadiazole as a corrosion inhibitor for mild steel in normal sulfuric acid medium". *Corros. Sci.* 48: 2831–2842.
- [109] Chitra S, Parameswari K, Sivakami C, Selvaraj A (2010). "Sulpha Schiff Bases as Corrosion Inhibitors for Mild Steel in 1M Sulphuric Acid". *Chem. Eng. Res. Bull.* 14: 1–6.
- [110] Afidah AR, Kassim J (2008). "Recent Development of Vegetal Tannins in Corrosion Protection of Iron Recent Patents Mater. Sci. 1: 223–231.
- [111] Umoren SA, Solomon MM, Udoso II, Udoh AP (2010). "Synergistic and antagonistic effects between halide ions and carboxy methyl cellulose for the corrosion inhibition of mild steel in sulphuric acid solution". *Cellulose* 17: 635–648.
- [112] Solomon MM, Umoren SA, Udoso II, Udoh AP (2010). "Inhibitive and adsorption behaviour of carboxy methyl cellulose on mild steel corrosion in sulphuric acid solution". *Corros. Sci.* 52 (4): 1317–1325.
- [113] Umoren SA, Obot IB, Ebenso EE, Obi-Egbedi NO (2009). "The Inhibition of aluminium corrosion in hydrochloric acid solution by exudate gum from *Raphiahookeri*". *Desalination* 247: 561–572.
- [114] Umoren SA, Obot IB, Obi-Egbedi NO (2009). "Raphiahookeri gum as a potential eco-friendly inhibitor for mild steel in sulphuric acid". *J. Mater. Sci.* 44: 274–279.
- [115] Mylius FZ (1922). "Der Aufbau der Zweistofflegierungen - Eine kritische Zusammenfassung. *Metallkunde.* 14: 233.
- [116] Aziz K, Shams El-Din AM (1965). "A simple method for the determination of the inhibition efficiency of surfactants". *Corros. Sci.* 5: 489.
- [117] Mylius F Z (1924). "Der Aufbau der Zweistofflegierungen - Eine kritische Zusammenfassung *Metallkunde.* 16: 81.
- [118] Fouda AS, El-Asmy AA (1987). "Efficiency of some phenyl thio semi carbazide derivatives in retarding the dissolution of aluminum in NaOH solution". *Monatsh. Chem.* 118: 709.
- [119] Morad MS, Kamal El-Dean AM (2006). "2,2'-Dithiobis(3-cyano-4,6-dimethylpyridine): A new class of acid corrosion inhibitors for mild steel". *Corros. Sci.* 48: 3398.
- [120] Becke AD (1993). "Density-functional thermochemistry. III. The role of exact exchange". *J. Chem. Phys.* 98: 5648–5652. Bib code: 1993JChPh..98.5648B. doi:10.1063/1.464913

- [121] (a) Becke AD (1988). "Density-functional exchange-energy approximation with correct asymptotic behavior". *Phys. Rev. A* 38:30983098–3100. Bibcode: 1988PhRvA...38.3098B; Lee. (b) Lee C, Yang W, Parr G G (1988). —Development of the Colle-Salvetti correlation-energy formula into a functional of the electron density. *Phys. Rev. B* 37 (2):785-789.
- [122] Frisch M J, Trucks G W, Schlegel H B, Scuseria G E, Robb M A M, Cheeseman J R, Montgomery J A, Vreven Jr T, Kudin K N, Burant J C, Millam J M, Iyengar S S, Tomasi J, Barone V, Mennucci B, Cossi M, Scalmani G, Rega N, Petersson GA, Nakatsuji H, Hada M, Ehara M, Toyota K, Fukuda R, Hasegawa J, Ishida M, Nakajima T, Honda Y, Kitao O, Nakai H, Klene M, Li X, Knox J E, Hratchian H P, Cross J B, Adamo C, Jaramillo J, Gomperts R, Stratmann RE, Yazyev O, Austin AJ, Cammi R, Pomelli C, Ochterski JW, Ayala PY, Morokuma K, Voth GA, Salvador P, Dannenberg JJ, Zakrzewski VG, Dapprich S, Daniels AD, Strain MC, Farkas O, Malick DK, Rabuck AD, Raghavachari K, Foresman JB, Ortiz JV, Cui Q, Baboul AG, Clifford S, Cioslowski J, Stefanov BB, Liu G, Liashenko A, Piskorz P, Komaromi I, Martin RL, Fox DJ, Keith T, Al-Laham MA, Peng CY, Nanayakkara A, Challacombe M, Gill PMW, Johnson B, Chen W, Wong MW, Gonzalez C, Gaussian 03 Pople JA (2004). —Supporting Information. Inc. Gaussian: Wallingford, CT.
- [123] Glendening E D, Reed AE, Carpenter JE, Weinhold F, version 3.1 NBO (1998). TCI, University of Wisconsin, Madison.
- [124] Chermette H (1999). "Chemical reactivity index χ reactivity indices in density functional theory". *J. Comput. Chem.* 20: 129–154.
- [125] Parr RG, Yang W (1989). "Density Functional Theory of Atoms and Molecules". Oxford University Press, Oxford.
- [126] Juric BS (1996). — Computation of electron affinities of O and F atoms, and energy profile of F–H₂ reaction by density functional theory and ab initio methods. *J. Chem. Phys.* 104: 4151–4157. ; <http://dx.doi.org/10.1063/1.471226>
- [127] Parr RG, Yang W (1984). "Density functional approach to the frontier-electron theory of chemical reactivity". *J. Am. Chem. Soc.* 106: 4049–4050.
- [128] Pearson RG (1963). "Hard and soft acids and bases". *J. Am. Chem. Soc.* 85:3533–3539.
- [129] Gece G (2008). "The use of quantum chemical methods in corrosion inhibitor studies". *Corros. Sci.* 50: 2981-2992.
- [130] Murrell JN, Kettle SF, Tedder JM (1985). *The Chemical Bond*, John Wiley and Sons, Chichester.
- [131] Grüber C, Buss V (1989). "Quantum-mechanically calculated properties for the development of quantitative structure-activity relationships (QSAR's). pKa-values of phenols and aromatic and aliphatic carboxylic acids". *Chemosphere* 19: 1595–1609.
- [132] Fang J, Li J (2002). "Quantum chemistry study on the relationship between molecular structure and corrosion inhibition efficiency of amides". *J. Mol. Struct. (Theochem)* 593: 179–185.
- [133] Lashkari M, Arshadi MR (2004). "DFT studies of pyridine corrosion inhibitors in electrical double layer: solvent, substrate, and electric field effects". *J. Chem. Phys.* 299: 131–138.
- [134] Sein LT, Wei Y, Jansen SA (2001). "The role of adsorption of aniline trimers on the corrosion inhibition process: a ZINDO/1 study". *Comput. Theor. Polym. Sci.* 11: 83–90.
- [135] Ebenso EE, Arslan T, Kandemirli F, Caner N, Love I (2010). "Quantum chemical studies of some rhodanine azosulpha drugs as corrosion inhibitors for mild steel in acidic medium". *Int. J. Quant. Chem.* 110: 1003–1018.
- [136] Gece G, Bilgic S (2010). "A theoretical study on the inhibition efficiencies of some amino acids as corrosion inhibitors of nickel". *Corros. Sci.* doi:10.1016/j.corsci.2010.06.015.
- [137] Fukui K (1975). *Theory of Orientation and Stereo selection*, Springer-Verlag, New York.
- [138] Lewis DFV, Ioannides C, Parke DV (1994). "Interaction of a series of nitriles with the alcohol-inducible isoform of P450: Computer analysis of structure-activity relationships". *Xenobiotica* 24 : 401–408.
- [139] Zhou Z, Parr RG (1990). "Activation hardness: New index for describing the orientation of electrophilic aromatic substitution". *J. Am. Chem. Soc.* 112: 5720–5724.
- [140] Pearson RG (1989). "Absolute electronegativity and hardness: applications to organic chemistry". *J. Org. Chem.* 54:1423–1430.
- [141] Hohenberg P, Kohn W (1964). "Inhomogeneous electron gas". *Phys. Rev.* 136: B864–871.
- [142] Kikuchi O (1987). "Systematic QSAR procedures with quantum chemical descriptors". *Quant. Struct.-Act. Relat.* 6 : 179–184.
- [143] Khaled KF, Fadl-Allah SA, Hammouti B (2009). "Some benzotriazole derivatives as corrosion inhibitors for copper in acidic medium: Experimental and quantum chemical molecular dynamics approach". *Mater. Chem. Phys.* doi:10.1016/j.matchemphys.2009.05.043.
- [144] Gece G (2008). "The use of quantum chemical methods in corrosion inhibitor studies". *Corros. Sci.* 50: 2981-2992.
- [145] Dwivedi A, Misra N (2010). "Quantum chemical study of Etodolac (Lodine)". *Der PharmaChemica.* 2(2): 58-65.
- [146] Sastri VS, Perumareddi JR (1997). "Molecular Orbital Theoretical Studies of Some Organic Corrosion Inhibitors". *Corrosion* 53: 617–622.
- [147] Lukovits I, Ka'ima' n E, Zucchi F (2001). "Corrosion Inhibitors—Correlation between Electronic Structure and Efficiency". *Corrosion* 57: 3–8.
- [148] Masoud MS, Awad MK, Shaker MA, El-Tahawy MMT (2010). "The role of structural chemistry in the inhibitive performance of some aminopyrimidines on the corrosion of steel". *Corros. Sci.* 52: 2387–2396.
- [149] Parr RG, Szentpaly L, Liu S (1999). "Investigation of substituent effect on carbene ligands". *J. Am. Chem. Soc.* 121: 1922–1928.
- [150] Wang H, Wang X, Wang H, Wang L, Liu A (2007). "DFT Study of New Bipyrazole Derivatives and Their Potential Activity as Corrosion Inhibitors". *J. Mol. Model.* 13: 147–153.
- [151] Chattaraj PK, Maiti B, Sarkar U (2003). "Philocity: A unified treatment of chemical reactivity and selectivity". *J. Phys. Chem. A* 107: 4973–4975.
- [152] Li X, Deng S, Fu H, Li T (2009). —Adsorption and inhibition effect of 6- benzylaminopurine on cold rolled steel in 1.0 M HCl. *Electrochim. Acta* 54: 4089–4098.
- [153] Abiola OK, Otaigbe JOE (2009). "The effects of Phyllanthus amarus extract on corrosion and kinetics of corrosion process of aluminum in alkaline solution". *Corros. Sci.* doi:10.1016/j.corsci. 2009.07.006.
- [154] Ebbing DD, Gammon SD (2005). *General Chemistry 8/e*, Houghton Mifflin, Boston, Massachusetts.
- [155] Abiola OK (2006). "Adsorption of 3-(4-amino-2-methyl-5-pyrimidylmethyl)-4-methyl thiazolium chloride on mild steel". *Corros. Sci.* 48:3078–3090.
- [156] Atkins P, de Paula J (2002). *A Textbook of Physical Chemistry*, seventh ed., University Press, Oxford : 873.
- [157] Quraishi MA, Rafiquee MZA, Khan S, Saxena N (2007). "Corrosion inhibition of aluminium in acid solutions by some imidazoline derivatives". *J. Appl. Electrochem.* 37: 1153–1162.
- [158] Bouklah M, Hammouti B, Lagrenee M, Bentiss F (2006). "Thermodynamic properties of 2,5-bis(4-methoxyphenyl)-1,3,4-oxadiazole as a corrosion inhibitor for mild steel in normal sulfuric acid medium". *Corros. Sci.* 48: 2831–2842.
- [159] Atkins PW (1998). *Physical Chemistry* : 6th edn. Oxford University Press, Oxford.
- [160] Migahed MA (2005). "Electrochemical investigation of the corrosion behaviour of mild steel in 2 M HCl solution in presence of 1-dodecyl-4-methoxy pyridinium bromide". *Mater. Chem. Phys.* 93: 48–53.
- [161] Cases JM, Villieras F (1992). "Thermodynamic model of ionic and nonionic surfactants adsorption-adsorption on heterogeneous surfaces". *Langmuir* 8: 1251–1264.
- [162] Tang L, Li X, Si Y, Mu G, Liu G (2006). "The synergistic inhibition between 8-hydroxyquinoline and chloride ion for the corrosion of cold rolled steel in 0.5 M sulfuric acid". *Mater. Chem. Phys.* 95: 29–38.

- [163] Sibel Z, Dogan P, Yazici B (2005) "Acidic corrosion of iron and aluminum by SDBS at different temperatures". *Corros.Rev.* 23: 217.
- [164] Musa AY, Kadhun AAH, Mohamad AB, Daud AR, TakriffMS, Kamarudin SK (2009). "A comparative study of the corrosion inhibition of mild steel in sulphuric acid by 4,4-dimethylloxazolidine-2-thione". *Corros. Sci.* 51: 2393–2399.
- [165] Benali O, Larabi L, Traisnel M, Gengembra L, Harek Y (2007). "Corrosion inhibition efficiency and surface activity of benzothiazol-3-ium cationic Schiff base derivatives in hydrochloric acid". *Appl. Surf.Sci.* 253: 6130–6137.
- [166] Noor EA, Al-Moubaraki AH (2008). "Thermodynamic study of metal corrosion and inhibitor adsorption processes in mild steel/1-methyl-4[4'(X)-styrylpyridinium iodides/hydrochloric acid systems". *Mater.Chem. Phys.* 110: 145–154.
- [167] Donahue FM, Nobe K (1965). "08_chapter 1. - Shodhganga". *J. Electrochem. Soc.* 112: 886–891. shodhganga.inflibnet.ac.in/.../8/08_chapter%201
- [168] Kamis E, Belluci F, Latanision RM, El-Ashry ESH (1991). "Inhibition of Nickel by 2-(Triphenosporanylidene) Succinic Anhydride". *Corrosion* 47(9): 677–686.
- [169] Yadav DK, Maiti B, Quraishi MA (2010). "Electrochemical and quantum chemical studies of 3,4-dihydropyrimidin-2(1H)-ones as corrosion inhibitors for mild steel in hydrochloric acid solution". *Corros. Sci.* 52: 3586–3598.
- [170] Badawy WA, Ismail KM, Fathi AM (2006). "Corrosion control of Cu–Ni alloys in neutral chloride solutions by amino acids". *Electrochim. Acta* 51: 4182–4189.
- [171] Abdallah M (2002). "Rhodanineazosulpha drugs as corrosion inhibitors for corrosion of 304 stainless steel in hydrochloric acid solution". *Corros. Sci.* 44: 717–728.
- [172] El-Awady AA, Abd-El-Nabey BA, Aziz SG, Khalifa M, Al-Ghamedy HA (1990). "Kinetics and Thermodynamics of the Inhibition of the Acid Corrosion of Steel by Some Macrocyclic ligands". *International J.Chem.* 1(4): 169–179.
- [173] El-Awady AA, Abd-El-Nabey BA, Aziz SG (1992). —Kinetic- Thermodynamic and Adsorption Isotherms Analyses for the Inhibition of the Acid Corrosion of Steel by Cyclic and Open- Chain Amines. *J. Electrochem.Soc.* 139 (8): 2149–2154.
- [174] Frumkin AN (1925). "Surface tension curves of higher fatty acids and the equation of condition of the surface layer". *Z. Phys. Chem.*, 116: 466–484.
- [175] Fouda AS, Mousa MNH, Taha FI, El-Neanaa AI (1986). "The role of some thiosemicarbazide derivatives in the corrosion inhibition of aluminum in HCl". *J. Corrosion. Sci.* 26: 719.
- [176] Langmuir I (1918). "The adsorption of gases on plane surface of glass, mica and platinum". *J. Amer. Chem. Soc.* 40:1361–1403.
- [177] Szkarska- Smialowska Z, Dus B (1967). "Effect of Some Organic Phosphorus Compounds on the Corrosion of Low Carbon Steel in Hydrochloric Acid Solutions". *Corrosion* 23: 130.
- [178] Ahamad I, Prasad R, Quraishi MA (2010). —Thermodynamic, electrochemical and quantum chemical investigation of some Schiff bases as corrosion inhibitors for mild steel in hydrochloric acid solutions. *Corros. Sci.* 52: 933.
- [179] Yurt A, Balaban A, UstünKandemir S, Bereket G, Erk B (2004). "Investigation on some Schiff bases as HCl corrosion inhibitors for carbon steel". *Mater. Chem. Phys.* 85: 420–426.
- [180] Vracar L, Drazic DM (2002). —Adsorption and corrosion inhibitive properties of some organic molecules on iron electrode in sulfuric acid. *Corros. Sci.* 44:1669–1680.
- [181] Soltani N, Behpour M, Ghoreishi SM, Naeimi H (2010). "Corrosion inhibition of mild steel in hydrochloric acid solution by some double Schiff bases". *Corros. Sci.* 52: 1351.
- [182] Hasanov R, Sadikog̃lu M, Bilgiç S (2007). "Electrochemical and quantum chemical studies of some Schiff bases on the corrosion of steel in H₂SO₄ solution". *Appl. Surf. Sci.* 253: 3913–3921.
- [183] Shokry H, Sekine I, Yuasa M, El- Baradie HY, Comma G K, Issa RM (1997). "Inhibition effect of Schiff base compounds on the corrosion of iron in nitric acid and sodium hydroxide solutions". *Zairyo to Kankyo.* 47 (7): 447.
- [184] Zhang QB, Hua YX (2009). "Corrosion inhibition of mild steel by alkylimidazolium ionic liquids in hydrochloric acid". *Electrochim. Acta* 54 (6): 1881–1887.
- [185] Keles H, Keles M, Dehri I, Serindag̃ O (2008). "The inhibitive effect of 6-amino-m-cresol and its Schiff base on the corrosion of mild steel in 0.5M HCl medium". *Mater. Chem. Phys.* 112: 173–179.
- [186] Solmaz R, Kardas G, Yazıcı B, Erbil M (2005). "Inhibition effect of rhodanine for corrosion of mild steel in hydrochloric acid solution". *Prot. Met.* 41: 581–585.
- [187] Kardas G (2005). —The Inhibition Effect of 2-Thiobarbituric Acid on the Corrosion Performance of Mild Steel in HCl Solutions. *Mater. Sci.* 41(3): 337–343
- [188] Ebenso EE, Oguzie EE (2005). "Corrosion inhibition of mild steel in acidic media by some organic dyes". *Mater. Lett.* 59: 2163–2165.
- [189] Aytac A, Özmen Ü, Kabasakalog̃lu M (2005). —Investigation of the inhibition effect of 5-(E)-4-phenylbuta-1,3-dienylideneamino)-1,3,4-thiadiazole-2-thiol Schiff base on mild steel corrosion in hydrochloric acid. *Mater. Chem. Phys.* 89: 176–181.
- [190] Solmaz R, Kardas G, Yazıcı B, Erbil M (2008). "Adsorption and corrosion inhibitive properties of 2-amino-5-mercapto-1,3,4-thiadiazole on mild steel in hydrochloric acid media". *Colloid Surf. A* 312: 7–17.
- [191] Li Y, Zhao P, Liang Q, Hou B (2005). "Berberine as a natural source inhibitor for mild steel in 1 M H₂SO₄". *Appl. Surf. Sci.* 252: 1245–1253.
- [192] Kaim W, Schwederski B, Heilmann O, Hornung FM (1999). "Coordination Compounds of Pteridine, Alloxazine and Flavine Ligands: Structures and Properties". *Coord. Chem. Rev.* 182 (1): 323–333.